Università degli Studi di Padova

Dipartimento di Biologia

Corso di Laurea Magistrale in Biotecnologie Industriali

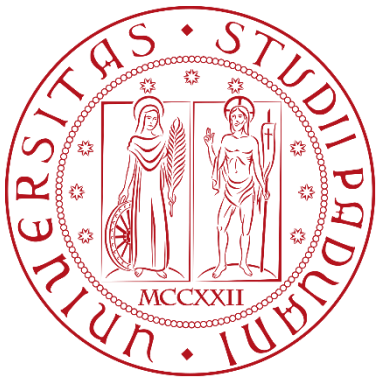

Engineering of lipid metabolism in the microalgae *Nannochloropsis gaditana*

Relatore: Prof. Tomas Morosinotto

Dipartimento di Biologia

Controrelatore: Prof.ssa Paola Venier

Dipartimento di Biologia

Laureando: Carlo Pilotto

Anno Accademico 2022/2023

Summary

Abstract

The exponential growth of the world population is causing an increased demand for energy and food that cannot be supported by current agricultural yields. Furthermore, intensive agriculture is the cause of strong environmental impacts, leading to soil degradation, loss of ecosystems and biodiversity. In this context, microalgae industrial cultivations will play a fundamental role in reducing the impacts of climate change and developing a more sustainable economy.

Among known microalgae, *Nannochloropsis* have attracted considerable attention due to their ability to accumulate a large fraction of reduced carbon as lipids. This master's thesis deals with the comprehension of microalgae lipid metabolism, with a particular focus on enhancing lipid accumulation in *Nannochloropsis gaditana*.

The central hypothesis driving this research is that modulation of a triose phosphate translocator (TPT) activity can lead to an increase in the cytosolic lipid content in specific growth conditions, because the principal triose phosphate molecule transported by this transporter is dihydroxyacetone phosphate (DHAP) that is also an essential molecule in the metabolism, being an intermediate in various metabolic pathways.

Through transcriptomic analysis, four genes encoding TPTs were previously identified in *Nannochloropsis gaditana* but only one of these transporters exhibit significant homology with an Apicomplexan-like DHAP transporter, which suggests a potential opposite role in lipid metabolism, importing DHAP from the cytosol to the chloroplast. To better understand the role of this transporter in the cell carbon partitioning, we used knockout mutants generated by CRISPR-Cas technology. A series of growth curve experiments were conducted to assess the impact of transporter disruption on neutral lipid accumulation.

Our findings demonstrate that the TPT knockout mutants exhibit a significant increase in lipid accumulation compared to the wild type in the tested light condition. This research not only contributes to our understanding of microalgae lipid metabolism, but also presents a promising

starting point for enhancing lipid production through targeted genetic modifications.

As a side project, we used an optimized strain of *Nannochloropsis oceanica* (IMET1) to obtain a mutant with the aim to overexpress a specific fatty acid desaturase (ω3 FAD) involved in converting ω-6 fatty acids to ω-3 fatty acids to improve the fatty acid profile and the ω3/ω6 ratio enhancing its nutritional value and health benefits.

1. Introduction

1.1 Environmental sustainability of food production

The exponential growth of the world population, estimated to reach 10 billion by 2050[1], has triggered an unprecedented demand for energy and food. With the increase in the global population, the production of food must also increase and estimates, as reported in[2], indicate that this increase needs to be in the range of 70% to 100% more than current levels to meet the growing demand and the needs of future population. However, this will inevitably exacerbate numerous issues related to food production, particularly the environmental impact originated from this activity.

The impact of human activities on the environment is well-documented and food production is among the major factors disrupting ecosystems balance. Among other issues, food production-related activities lead to significant environmental impact in terms of greenhouse gas emissions.

For instance, land use for agriculture and livestock, which occupies roughly half of habitable land, is a leading cause of biodiversity loss. The use of monocultures or low-diversity livestock systems, rather than natural environments, results in genetic erosion. Moreover, the excessive use of fertilizers, aimed at maximizing yields and increasing production, leads to the rapid growth of certain plant species at the expense of others. This imbalance prevents some species from accessing light and nutrients, ultimately leading to their disappearance, which, in turn, affects the species that rely on them for sustenance. This further disrupts biodiversity, natural systems these factors exacerbate the problem of water body eutrophication caused by the excessive release of nutrients, including nitrogen, phosphorus, and other substances found in fertilizers, which are then leached from the soil and reach water bodies[3].

[1] Caporgno and Mathys, 'Trends in Microalgae Incorporation Into Innovative Food Products With Potential Health Benefits'.
[2] Godfray et al., 'Food Security'.
[3] Nellemann, United Nations Environment Programme, and GRID--Arendal, *The Environmental Food Crisis*.

The replacement of natural systems like forests and grasslands, which act as carbon sinks by absorbing CO_2 from the atmosphere, with pastures and cultivated lands also contributes to greenhouse gas emissions. These emissions, coupled with those caused by food production, supply chains, and food waste, all compound the environmental impact.

Another aspect linked to food production is water usage: agriculture is the most-consuming sector. This environmental footprint is naturally more pronounced in areas with limited water availability, as water scarcity varies around the world[4].

Overall, in the years to come, increased greenhouse gas emissions, raised competition for productive lands, water, and energy resources, combined with the overexploitation of ecosystems will strongly impact our ability to produce sufficient food[5].

The challenge presented is to find ways to produce quantities of food that can meet the ever-increasing demand while mitigating the negative effects of the food industry on the environment and ensuring equitable and sustainable food security (Figure 1).

In this context, microalgae are emerging as a sustainable alternative for food production, due to their biomass composition, high photosynthetic rate and ability to grow on different substrates without consuming arable land. Microalgae do not compete with plants for arable land because they thrive without the need for fertile soils. This characteristic allows for the exploitation of marginal and non-productive areas, such as deserts. Also, their unique ability to proliferate in diverse aquatic environments, including seawater or even wastewater, makes them well-suited for cultivation in areas where traditional agriculture is challenging and playing a crucial role in bioremediation which makes their production even more sustainable by reducing the demand for energy, fertilizers and water.

[4] Ritchie, Rosado, and Roser, 'Environmental Impacts of Food Production'.
[5] Nellemann, United Nations Environment Programme, and GRID--Arendal, *The Environmental Food Crisis*.

Microalgae biomass contains proteins, but also various health-beneficial compounds, such as carbohydrates, polyunsaturated fatty acids, edible oils, essential minerals and vitamins. These elements enhance the nutritional value of food products obtained through industrial processes[6]. It is projected that by mid-century microalgae could represent 18% of the protein sources used by humans[7]. For these reasons, microalgae industrial cultivation will play a pivotal role in reducing the impacts of climate change and promoting a more sustainable economy.

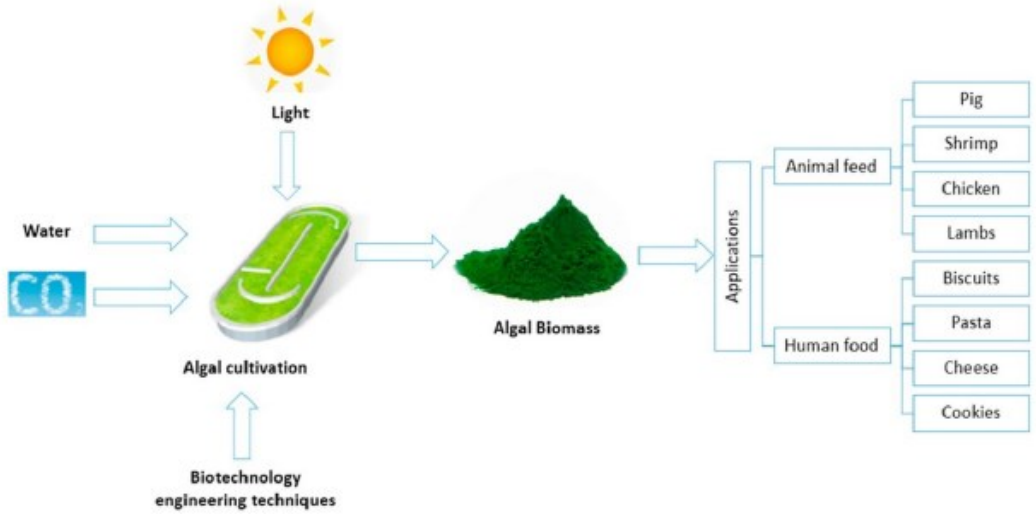

FIGURE 1: Graphical abstract concerning the possible products obtained by microalgae cultivation[8]

1.2 Microalgae: overview and applications

Microalgae are unicellular microorganisms with sizes ranging from 0.2 μm to slightly over 100 μm that thrive in the presence of sunlight, atmospheric CO_2 and nutrients present in the aquatic medium. They are eukaryotic organisms found in all ecosystems, colonizing freshwater, wastewater, and

[6] Xue et al., 'Research Advancement and Commercialization of Microalgae Edible Oil'.
[7] Van Der Spiegel, Noordam, and Van Der Fels-Klerx, 'Safety of Novel Protein Sources (Insects, Microalgae, Seaweed, Duckweed, and Rapeseed) and Legislative Aspects for Their Application in Food and Feed Production'.
[8] Kusmayadi et al., 'Microalgae as Sustainable Food and Feed Sources for Animals and Humans – Biotechnological and Environmental Aspects'.

marine environments[9]. Some species can even endure extreme conditions, withstanding high temperatures, varying pH levels, and elevated CO_2 concentrations.

These photosynthetic organisms, through photosynthesis, can convert solar radiation energy, absorbed through pigments, into chemical energy through photosystem I and photosystem II, two multiprotein complexes located in the thylakoid membranes of the chloroplast[10]. Overall, they synthesize carbohydrates from carbon dioxide (CO_2) while water (H_2O) is oxidised, releasing oxygen (O_2) as a byproduct. Remarkably, microalgae are responsible for approximately 50% of global photosynthesis and atmospheric oxygen production[11].

Photosynthesis can be divided into two phases: the light-dependent phase and the metabolic phase (carbon fixation by Calvin-Benson cycle). In the light phase, light energy is transformed into chemical energy and reducing power in the form of ATP and NADPH. In the metabolic phase, ATP and NADPH are used for carbon fixation from CO_2.

In recent years, microalgae have gained attention as potential sources of food, biofuels, cosmetic ingredients and nutraceuticals, among other applications. They offer environmental sustainability advantages over traditional plants as they do not require arable land, making it possible to cultivate them in marginal and unproductive areas like deserts[12]. Unlike plants, they do not need freshwater to grow and can thrive in seawater or wastewater, being excellent candidates also for bioremediation applications. Indeed, their cultivation can mitigate pollution in waters contaminated with nitrogen and phosphorus, and they can act as sinks for industrial CO_2 emissions, contributing to reduce atmospheric emissions and

[9] Ravindran et al., 'Microalgae Potential and Multiple Roles—Current Progress and Future Prospects—An Overview'.
[10] Basso et al., 'Characterization of the Photosynthetic Apparatus of the Eustigmatophycean Nannochloropsis Gaditana'.
[11] Ma et al., 'Lipid Production from Nannochloropsis'.
[12] Paul Abishek, Patel, and Prem Rajan, 'Algae Oil'.

aligning with the principles of circular economy, which focuses on recycling materials to reduce waste and pollution.

Furthermore, microalgae outperform plants in terms of photosynthetic productivity due to higher carbon fixation efficiency and more efficient use of radiation (which varies among species). They do not experience seasonality, ensuring year-round productivity. Being unicellular organisms, they do not invest metabolic energy in non-photosynthetic tissues, such as plant roots, making the entire biomass photosynthetically active and simplifying industrial processing[13].

These organisms exhibit high growth rates and can produce a wide range of metabolites and biomolecules, including protein, carbohydrates, vitamins, antioxidants, polyunsaturated fatty acids (PUFAs), and pigments. Some species can accumulate lipids, ranging from 20% to 50% of dry weight, and up to 85% in specific growth conditions like nutrient limitation or high light intensity[14].

Given these numerous advantages, the interest in industrial microalgae production has led to the development of infrastructure aimed at maximizing production yields.

1.3 Microalgae cultivation

The large-scale cultivation of microalgae has been explored as a promising source of sustainable biomass for various applications, including food, animal feed, chemicals, biofuels, and high-value products. Currently, two primary mass-cultivation systems are employed: photobioreactors (PBRs) and open ponds (Figure 2). Closed PBRs offer better control over contamination and physiochemical conditions. However, they come with significantly higher capital, operational and energy costs compared to open

[13] Liu, Wang, and Feng, 'Effects of Reaction Parameter on Catalytic Hydrothermal Liquefaction of Microalgae into Hydrocarbon Rich Bio-Oil'.
[14] Xue et al., 'Research Advancement and Commercialization of Microalgae Edible Oil'.

raceway ponds, which are less complex and require lower initial investment [15].

Open ponds typically have depths ranging from 1 to 100 cm and are often equipped with agitators to facilitate the circulation of gases and nutrients within the culture. While pond cultivation is advantageous from an energy and economic perspective, it is subject to environmental variations, thus posing challenges in terms of growth factors control. In particular, CO_2 diffuses directly from the atmosphere, and light levels often vary with changing seasons, time of day, and weather conditions. Additionally, the open design makes these ponds susceptible to external contaminations and results in continuous evaporation, limiting overall productivity despite the large area occupied.

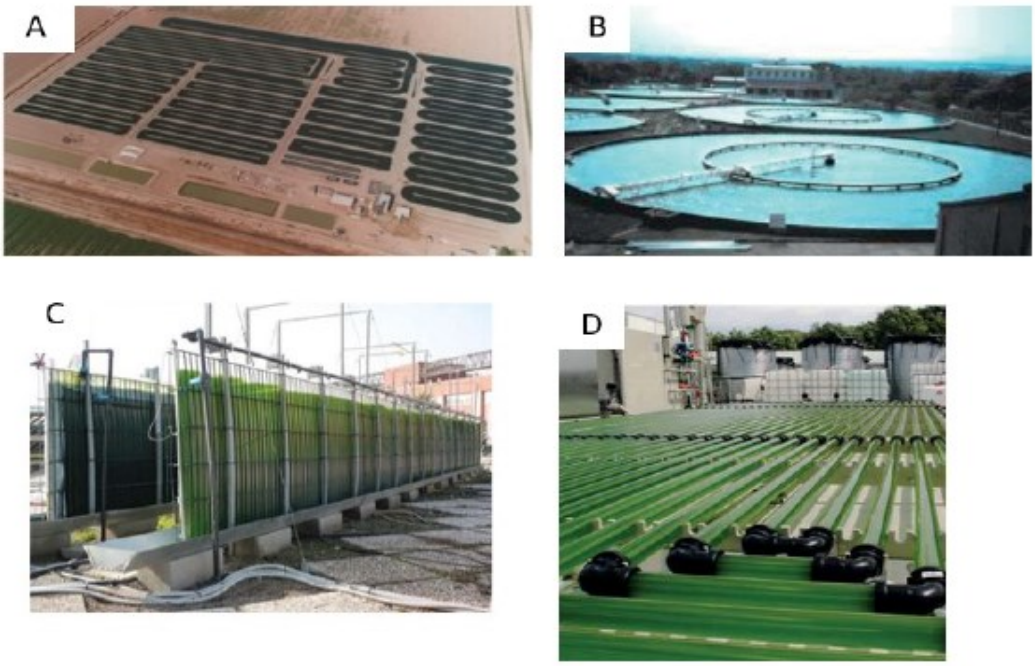

FIGURE 2: Microalgae industrial cultivation methods. A and B: examples of open ponds; C and D: examples of photobioreactors[16]

[15] Dolganyuk et al., 'Microalgae'.
[16] Maeda et al., 'Marine Microalgae for Production of Biofuels and Chemicals'; Razeghifard, 'Algal Biofuels'.

In contrast, photobioreactors are closed systems with various design options, usually made of transparent materials to allow light exposure, whether from natural sunlight or artificial sources. There are different types of photobioreactors, including bubble-airlift, bubble-column, tubular and panel photobioreactors (Figure 3). These systems are finely regulated by monitoring culture conditions, including temperature, pH, and nutrient flow. They can provide higher productivity yields but come with higher costs, increased energy consumption, and more complex maintenance requirements[17].

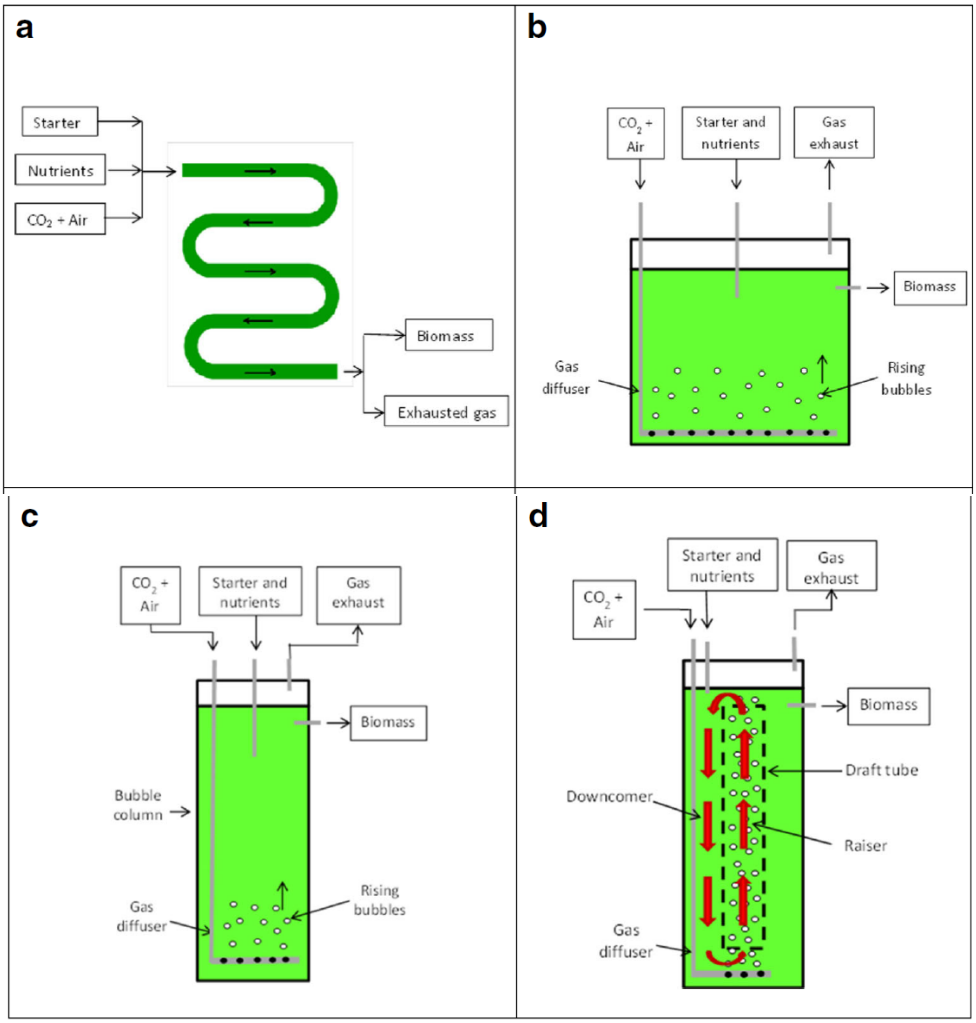

FIGURE 3: Conventional photobioreactors for algae cultivation. a Tubular. b Vertical airlift panel. c Bubble column. d Bubble airlift[18]

[17] Dolganyuk et al., 'Microalgae'.
[18] Santos-Sánchez et al., 'Lipids Rich in ω-3 Polyunsaturated Fatty Acids from Microalgae'.

Despite the numerous advantages of industrial algal cultivation, several limitations still impede its economic sustainability. Large-scale cultivation is costly, exceeding the expenses associated with plant cultivation, and current yields fall short of meeting global energy and food demands[19]. Biomass harvesting is a complex task since cultivation takes place in water, and once the growth cycle is complete, the water must be removed to concentrate the algal biomass. Harvesting the biomass is a highly energy-intensive and consequently expensive production step. Ongoing efforts are directed toward developing more efficient photobioreactors with optimized designs and regulation to maximize biomass yields and reduce production costs[20].

Table 6. Characteristics of possible methods for microalgae cultivation.

Cultivation Method	Energy Source	Carbon Source	Cell Biomass Accumulation Rate	Reactor Type	Price	Features
Phototrophic	Light	Inorganic	Low	Photobioreactor/ open waters	Low	The cell density of the culture is low; water evaporation
Heterotrophic	Organic matter	Organic	High	Bioreactor	Medium	The high price of the nutrient medium components; possibility of microbial contamination
Mixotrophic	Light, organic matter	Organic and inorganic	Medium	Closed photobioreactor	High	The high price of the nutrient medium components; possibility of microbial contamination

FIGURE 4: Characteristics of possible methods for microalgae cultivation[20]

1.4 Biomolecules from microalgae

The growth and biomass yield levels, as well as the micro- and macro-metabolites of microalgae, are predominantly influenced by environmental factors such as light, pH, temperature, and nutrients. Major metabolites within algal cells include proteins, carbohydrates, lipids, and other chemical compounds, e.g. pigments, essential minerals, and vitamins[21]. Microalgae

[19] Liu, Wang, and Feng, 'Effects of Reaction Parameter on Catalytic Hydrothermal Liquefaction of Microalgae into Hydrocarbon Rich Bio-Oil'.
[20] Dolganyuk et al., 'Microalgae'.
[21] Ravindran et al., 'Microalgae Potential and Multiple Roles—Current Progress and Future Prospects—An Overview'.

contain a diverse range of carbohydrates, including sugars, which serve both structural and metabolic roles. The most abundant ones are typically glucose, galactose and mannose, and they are synthesized within the chloroplast. These carbohydrates can be transformed into biofuels through various biochemical processes and by harnessing biomass conversion technologies such as anaerobic digestion, anaerobic fermentation and biological hydrogen production (Figure 5).

Regarding proteins, certain microalgae produce high levels of these molecules due to their capacity to synthesize all essential amino acids. The increasing demand for protein arising from the growing global population could in part be satisfied by the production of protein-based microalgae. In addition to the advantages previously mentioned, microalgae require significantly less land volume in comparison to the production of animal or plant-based proteins[22].

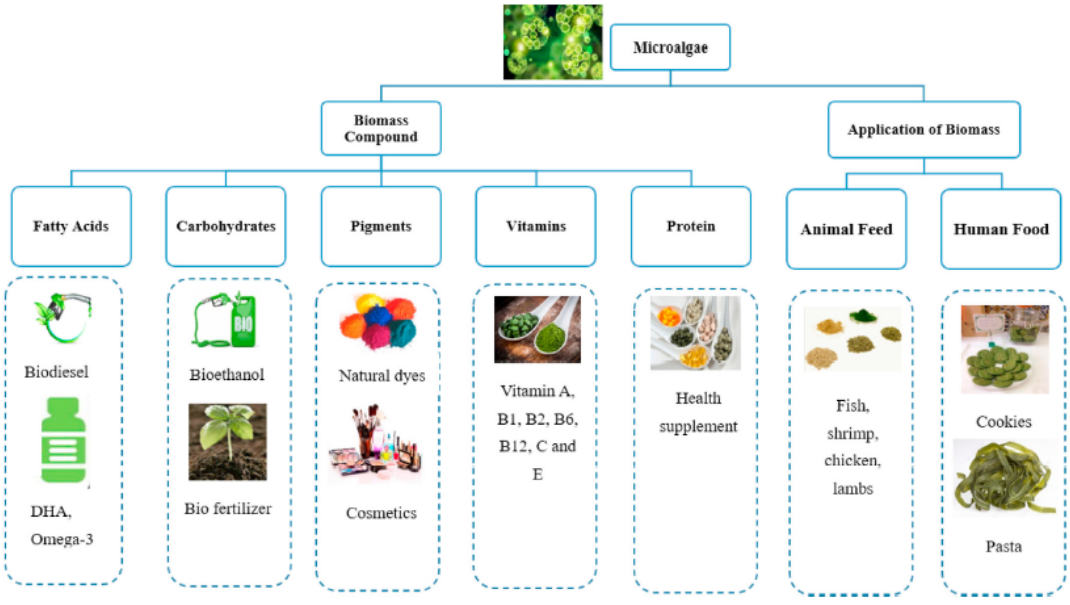

Fig. 1. Bioproducts acquired from algal biomass and their applications.

FIGURE 5: Bioproducts acquired from alga biomass and their application[23]

Microalgae contain various types of pigments: carotenoids, xanthophylls, phycobilins and chlorophylls, which can be used as antioxidants and anti-

[22] Caporgno and Mathys, 'Trends in Microalgae Incorporation Into Innovative Food Products With Potential Health Benefits'.
[23] Kusmayadi et al., 'Microalgae as Sustainable Food and Feed Sources for Animals and Humans – Biotechnological and Environmental Aspects'.

inflammatories, but also as dyes (Figure 6). The content of carotenoids and chlorophyll in microalgae is usually higher than in some plants. Microalgae also serve as a source of bioactive compounds, including minerals and vitamins like A, B1, B2, B6, B12, C, E, biotin, folic acid, pantothenic acid, potassium, iron, magnesium, calcium and iodine and many others, offering diverse health and nutritional benefits (Dolganyuk et al., 2020)[24]. This enhances the nutritional and commercial value of edible products in which they are incorporated. It has been demonstrated that they overcome common terrestrial crops in their capacity to provide these compounds [25].

Bioactive Compounds	Source	Health Benefits
Carotenoids		
β-carotene	*Dunaliella salina*	Antioxidant, pro-vitamin A, anti-allergic, anti-inflammatory
Astaxanthin	*Haematococcus pluvialis, C. zofingiensis*	Antioxidant, anti-inflammatory
Lutein	*Scenedesmus spp., Muriellopsis sp., C. sorokiniana*	Antioxidant, anti-inflammatory
PUFAs		
Arachidonic acid (AA)	*Porphyridium purpureum, P. cruentum, Parietochloris incisa*	Improves normal growth, visual and functional development in infants
Eicosapentaenoic acid (EPA)	*Nannochloropsis* sp., *Phaeodactylum tricornutum, Porphyridium cruentum*	Cardiovascular benefits, mental development and support, anti-inflammatory, protection against atherosclerosis
Docosahexaenoic acid (DHA)	*Crypthecodinium cohnii, Schizochytrium* spp., *Ulkenia* spp.	Cardiovascular benefits, improves nervous system development and function of the brain
Other metabolites		
Peptides	*Chlorella pyrenoidosa, Nannochloropsis oculata*	Antioxidant, anti-inflammatory, anticancer, antihypertensive
Phenolics	*Arthrospira maxima, Tetraselmis suecica, Botryococcus braunii, Isochrysis* sp., *Chlorella vulgaris, Nannochloropsis* sp.	Antioxidant
Phycocyanin	*Arthrospira platensis*	Antioxidant, anti-inflammatory
Sulfated polysaccharides	*C. pyrenoidosa, C. stigmatophora, Porphyridium* sp., *Phaeodactylum tricornutum*	antioxidant, anti-inflammatory, antiviral, immunomodulatory
"Water-soluble extract"	*Chlorella stigmatophora, Phaeodactylum tricornutum, Graesiella* sp.	Anti-inflammatory, analgesic, antioxidant, antiproliferative

FIGURE 6: Bioactive compounds from microalgae and their potential health benefits[26]

Overall, lipids represent a major component of animal feeds and play a pivotal role in the human diet. They are involved in a multitude of vital biological functions within the cell and are categorized into two groups: neutral lipids, including triacylglycerols (TAGs) and free fatty acids, and

[24] Dolganyuk et al., 'Microalgae'.
[25] Fawcett et al., 'Microalgae as an Alternative to Oil Crops for Edible Oils and Animal Feed'.
[26] Barkia, Saari, and Manning, 'Microalgae for High-Value Products Towards Human Health and Nutrition'.

polar lipids, such as phospholipids and glycolipids. Polar lipids have structural functions and are the primary constituents of membranes, whereas neutral lipids function as reserves and are usually found in lipid droplets. Long-chain polyunsaturated fatty acids (PUFAs) play an important role in human nutrition and are largely absent in oils derived from terrestrial plants[27]. These PUFAs, particularly those with extended carbon chains (20 or more carbon atoms), are bioactive substances falling into two main families, omega 3 (ω-3) and omega 6 (ω-6), characterized by their first double bond occurring at carbon atom positions 3 and 6, respectively (Figure 7). Eicosapentaenoic acid (EPA C20:5) and docosahexaenoic acid (DHA C22:6) are the ω-3 molecule more important because they have anti-inflammatory activity and exhibit a substantial positive effect in the prevention and treatment of heart and kidney diseases, brain development, metabolic regulation, and eye health [28].

These so-called “essential fatty acids” are not naturally produced by humans but are necessary and can be incorporated into the diet. For instance, they are found in fish, which in turn obtain them by consuming marine algae, the primary producers of these substances.

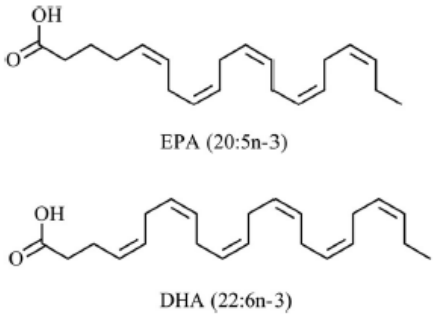

FIGURE 7: Chemical structure of EPA and DHA[29]

1.5 *Nannochloropsis*

Nannochloropsis is a genus of unicellular, non-motile marine microalgae belonging to the Eustigmatophyceae and distributed worldwide in marine, fresh and brackish waters, capable of significant lipid accumulation, especially under nutrient deprivation[30]. This genus comprises six known

[27] Santos-Sánchez et al., ‘Lipids Rich in ω-3 Polyunsaturated Fatty Acids from Microalgae’.
[28] Caporgno and Mathys, ‘Trends in Microalgae Incorporation Into Innovative Food Products With Potential Health Benefits’.
[29] Li-Beisson et al., ‘The Lipid Biochemistry of Eukaryotic Algae’.
[30] Alboresi et al., ‘Light Remodels Lipid Biosynthesis in *Nannochloropsis Gaditana* by Modulating Carbon Partitioning between Organelles’.

species: *Nannochloropsis gaditana*, *Nannochloropsis granulata*, *Nannochloropsis limnetica*, *Nannochloropsis oceanica* (Figure 8), *Nannochloropsis oculata*, and *Nannochloropsis salina*. Phylogenetically, it is a secondary endosymbiont, more closely related to brown algae and diatoms than to green algae. *Nannochloropsis* is a photoautotrophic organism, meaning it requires light energy to synthesize organic substances necessary for its growth and sustenance. Due to its high photosynthetic efficiency, this organism exhibits rapid growth, with growth rates ranging from 0.11 to 0.21 per day. Moreover, these growth rates have the potential to further increase under optimal growing conditions.

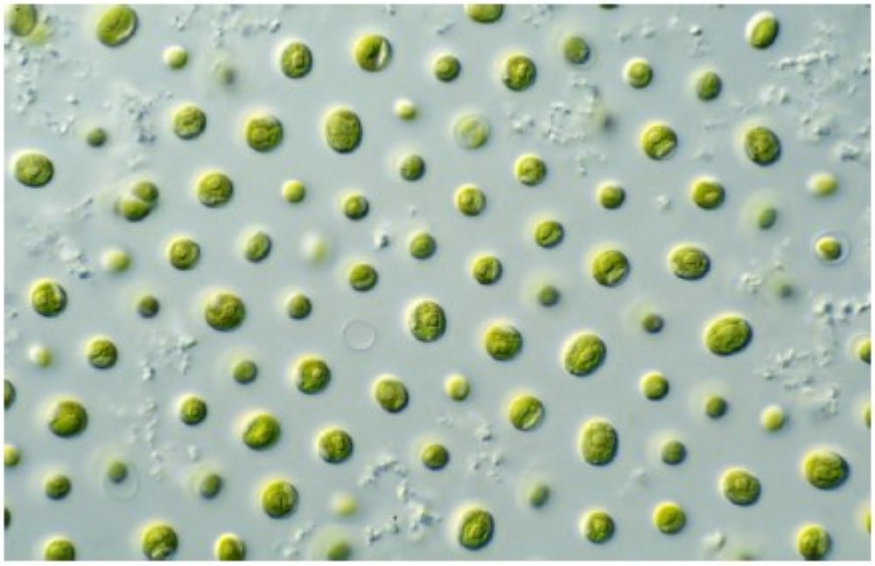

FIGURE 8: Microscope image of *Nannochloropsis oceanica* from the Commonwealth Scientific and Industrial Research Organization (CSIRO, https://www.csiro.au). *Nannochloropsis gaditana* optical microscopy image obtained from National Center for Marine Algae and Microbiota

Cells exhibit a simple spherical morphology with diameters ranging from 2 to 4 μm[31]. This class of microalgae originated from a secondary endosymbiosis event in which a eukaryotic progenitor engulfed a red alga[32]. This event resulted in the presence of four membranes surrounding the single chloroplast of the cell.

[31] Ma et al.
[32] Meneghesso et al., 'Photoacclimation of Photosynthesis in the Eustigmatophycean Nannochloropsis Gaditana'.

Nannochloropsis species possess a distinctive pigment composition, displaying chlorophyll *a* and lacking all other accessory chlorophyll molecules. While the most abundant carotenoids in *Nannochloropsis* are violaxanthin and vaucheraxanthin[33].

In the last decades, the microalgal genus *Nannochloropsis* has been gaining increasing research interest both for its ability to synthesize neutral lipids for biodiesel production and for its high content of polyunsaturated fatty acids (PUFAs), particularly the ω-3 fatty acid eicosapentaenoic acid (EPA, C20:5), that makes the biomass suitable for the production of these high value oils.

It is generally accepted that high growth rate, substantial lipid content, proper fatty acid composition, environmental adaptability, and resistance to contamination are desirable traits when screening microalgal candidates for lipid production. *Nannochloropsis* is considered a promising oleaginous model microalga due to its exceptional photosynthetic efficiency, high lipid productivity, well-established genetic tools and relatively mature technology for large-scale outdoor cultivation systems[32]. In particular, it has a lipid content ranging between 37% and 60% in dry weight, which is higher than many other microalgal strains. Additionally, the presence of numerous genes involved in lipid metabolism suggests a complex pathway regulation[34].

For these reasons, and due to its ability to produce valuable molecules, *Nannochloropsis* has significant potential for the production of edible oil, which could find applications in the food industry as a substitute or as an alternative to more common plant-derived oils[35].

[33] Lubián et al., '[No Title Found]'.
[34] Radakovits et al., 'Draft Genome Sequence and Genetic Transformation of the Oleaginous Alga Nannochloropsis Gaditana'.
[35] Ma et al., 'Lipid Production from Nannochloropsis'.

1.6 Fatty acid biosynthesis pathway

In all known eukaryotic species with a chloroplast, de novo fatty acids (FAs) synthesis is known to occur in the stroma. This process initiates through photosynthesis, whereby carbon dioxide (CO_2) is converted into glyceraldehyde-3-phosphate (G3P). G3P is subsequently transformed into pyruvate and, ultimately, into acetyl-CoA, thanks to the action of pyruvate dehydrogenase (PDH). Following this, acetyl-CoA undergoes an ATP-dependent conversion into malonyl-CoA, a reaction catalyzed by acetyl-CoA carboxylase (ACCase), an enzyme meticulously regulated. Indeed, the activity of ACCase plays a crucial role in controlling the flow of carbon into fatty acid synthesis and a positive correlation has been observed between ACCase activity and the quantity of fatty acids in photosynthetic organisms, including microalgae[36].

In the plastid, the malonyl-CoA is transferred to the acyl-carrier protein (ACP), which is one of the subunits of the type II fatty acid synthase (FASII) multiprotein complex. FASII allows a series of repetitive cycles, involving consecutive reduction, dehydration and reduction reactions. These cycles lead to the addition of two carbon atoms from malonyl-ACP in each iteration. Consequently, malonyl-ACP is attached to acetyl-CoA, forming 3-ketoacyl-ACP, facilitated by ketoacyl-ACP synthase (KAS), with the release of a molecule of CO_2. The resulting 4-carbon molecule then undergoes the three aforementioned reactions, catalyzed by FASII proteins, producing a saturated 4-carbon acyl molecule linked to ACP. This sequence of reactions is repeated seven times, ultimately yielding palmitoyl-ACP (C16:0-ACP).

This 16-carbon molecule, bound to ACP, can follow one of three paths: it can be acylated to glycerol within the chloroplast by a chloroplast-localized acyltransferase, constituting plastidial lipids. Alternatively, it can be "released" from ACP through the action of a thioesterase (FAT), interrupting chain elongation and generating a free fatty acid. The chain can also be further elongated by KASII to produce stearoyl-ACP (C18:0-ACP) by adding

[36] Li-Beisson et al., 'The Lipid Biochemistry of Eukaryotic Algae'.

two carbon atoms from acetyl-CoA. C16:0 and C18:0 still bound to ACP can be subjected to desaturation by stromal-ACP desaturase (SAD), yielding palmitoleic (C16:1) or oleic acid (C18:1). A thioesterase, located in the chloroplast stroma, can catalyze the removal of the ACP group from the 18-carbon chain, whether it has undergone desaturation or not, similar to what occurs with 16-carbon fatty acids. The products resulting from the thioesterase and desaturase activities are then transported to the cytosol, where they act as a cytosolic pool of free fatty acids (Figure 9). They can be transferred to the endoplasmic reticulum (ER), where further reactions of fatty acid condensation, elongation, and desaturation occur, leading to the formation of phospholipids and neutral lipids. Acyl chains can also remain in the plastid for the synthesis of structural lipids in the thylakoids, primarily glycolipids[37].

The synthesis of polyunsaturated fatty acids (PUFAs) requires the activity of specific elongases and desaturases, primarily acting on palmitic, stearic, and oleic acids. Fatty acid elongation occurs in both plastids and the ER, necessitating acyl-CoA and malonyl-CoA as substrates, as well as one molecule of ATP and two molecules of NADPH for every 2 added carbon atoms in the chain. The elongase responsible for the formation of long-chain fatty acids like eicosapentaenoic acid (EPA) and docosapentaenoic acid (DHA) is the elongase of very-long-chain fatty acids (ELOVL), present in *Nannochloropsis gaditana* and the majority of marine microalgae[38].

Desaturases are enzymes with a key role in shaping the organism lipid composition and determining the abundance of different fatty acid classes. These enzymes are specialized in introducing double bonds at specific positions in defined-length fatty acid chains and reaction catalyze by them require NADPH as an electron donor[38].

Acyl-ACP desaturases are soluble enzymes located in the plastids of higher plants, while stromal-ACP desaturases are located in the chloroplast and act on palmitic acid (C16:0), converting it into palmitoleic acid (C16:1) or

[37] Bellou et al., 'Microalgal Lipids Biochemistry and Biotechnological Perspectives'.
[38] Li-Beisson et al., 'The Lipid Biochemistry of Eukaryotic Algae'.

stearic acid (C18:0), converting it into oleic acid (C18:1). Other desaturases located in the endoplasmic reticulum gradually introduce double bonds in acyl chains during elongation, resulting in the formation of PUFAs.

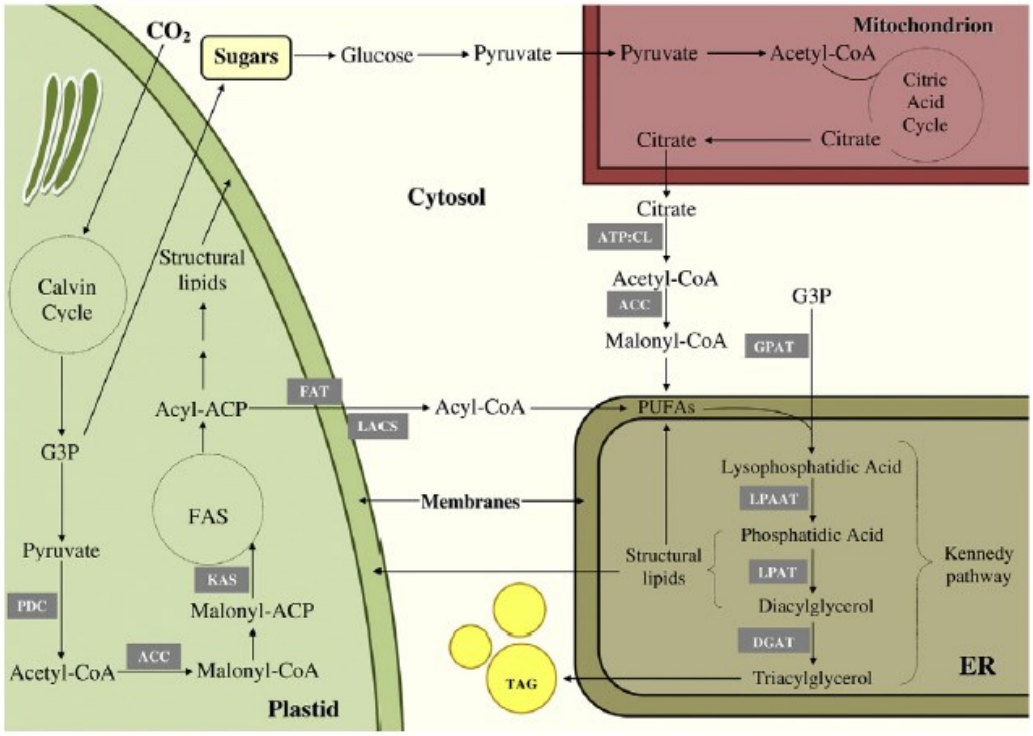

FIGURE 9: Simplified scheme showing lipid synthesis in microalgae[39]

1.7 TAG biosynthesis

Triacylglycerols (TAGs) are a type of lipid molecule that serves as a major storage form of energy. They are composed of three fatty acid molecules esterified to a glycerol molecule. When the organism needs energy TAGs can be hydrolyzed to release fatty acids, which are then used for energy production. Some microalgal species excel at accumulating triacylglycerols (TAGs) in lipid bodies within the cytosol, thanks to a highly coordinated metabolic pathway that spans the chloroplast, endoplasmic reticulum, and cytosol itself[40].

[39] Bellou et al., 'Microalgal Lipids Biochemistry and Biotechnological Perspectives'.
[40] Alboresi et al., 'Light Remodels Lipid Biosynthesis in *Nannochloropsis Gaditana* by Modulating Carbon Partitioning between Organelles'.

Multiple pathways for TAG biosynthesis have been described in different organisms and tissues, the Kennedy is the canonical pathway leading to TAG synthesis (Figure 10). In this pathway, the biosynthesis of TAG occurs through successive acylation reactions, that terms with the conversion of diacylglycerol (DAG) into TAG through the action of acylCoA:diacylglycerol acyltransferase (DGAT)[41].

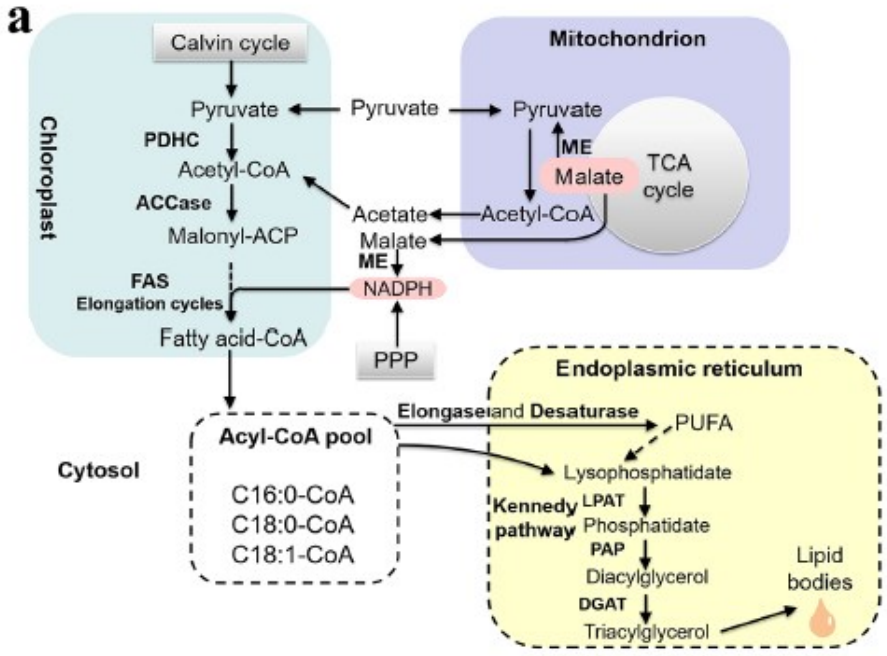

FIGURE 10: Lipid biosynthesis pathway in *Nannochloropsis*[42]

Nannochloropsis stands out as an interesting model for studying the regulation of metabolic fluxes towards lipids or carbohydrates synthesis, also through the genomic enrichment of biosynthesis genes, that supports its ability to synthesize lipids.

One example is the Diacylglycerol acyltransferase-2 (DGAT-2) genes, which in *Nannochloropsis* species showed 11 copies against the 4 or 5

[41] Turchetto-Zolet et al., 'Diversity and Evolution of Plant Diacylglycerol Acyltransferase (DGATs) Unveiled by Phylogenetic, Gene Structure and Expression Analyses'.
[42] Ma et al., 'Lipid Production from Nannochloropsis'.

copies present in other organism like diatoms or *Chlamydomonas* despite all having much larger genomes than *Nannochloropsis*[43].

A well-studied condition that triggers lipid accumulation in several algal species is represented by nitrogen depletion. However, this nutrient deficiency has some negative aspect that influence and reduce basic metabolic functions, including nucleic acid and protein biosynthesis, cell division and growth. Consequently, exploring alternative triggers for TAG biosynthesis, without compromising biomass growth, is a valuable pursuit.

The response of *Nannochloropsis gaditana* to light intensity has been already investigated, showing that light intensity can induce lipid accumulation[44]. In particular, those results revealed that high light leads to lipid accumulation through the coordinated activation of cytosolic fatty acid synthase of type 1 (FAS1) and contemporary inhibition of chloroplast fatty acid synthase of type 2 (FAS2). This process redirects the carbon flux out of the chloroplast and towards the ER, thus promoting TAG accumulation.

Interestingly, inside the cells, in low light condition (LL) than to medium light (ML) and high light (HL), one carbohydrate intermediate is more abundant than others: dihydroxyacetone phosphate (DHAP)[44]. DHAP is an essential molecule in the metabolism, being an intermediate in various metabolic pathways located in different compartments of the cell. Indeed, during glycolysis, hexose phosphates are broken-down into three-carbon intermediates: DHAP and GAP (glyceraldehyde 3-phosphate), two compounds that can be interconverted by the action of an isomerase (Figure 11).

Based on these considerations, the subcellular compartmentalization of enzymes involved in DHAP production and consumption, as well as the trafficking of DHAP between compartments, appear to play an important role in regulating carbon metabolic fluxes and partitioning. These

[43] Alboresi et al., 'Light Remodels Lipid Biosynthesis in *Nannochloropsis Gaditana* by Modulating Carbon Partitioning between Organelles'.

observations raise the interesting idea that DHAP could be a checkpoint for metabolic reprogramming towards lipid biosynthesis[44].

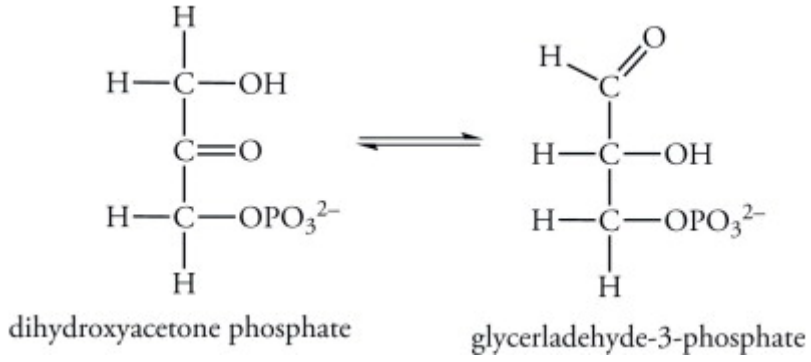

FIGURE 11: Interconversion between DHAP and GAP (Ouellette et al., 2014)[45]

1.8 TPT transporter

Given its potentially crucial role in carbon fluxes regulation, it is important to understand the triose phosphate transporter (TPT) functioning and explore possible manipulation strategies.

In primary chloroplasts, TPT transporters facilitate the export of dihydroxyacetone phosphate (DHAP) to the cytosol in exchange for inorganic phosphate (Pi), essential for ATP regeneration in the stroma. In contrast, in secondary plastids of Apicomplexa, non-photosynthetic organisms presenting a plastid enclosed by four membranes, TPT transporters act in an opposite way, importing DHAP in the plastid to support fatty acid synthesis.

A transcriptomic analysis of *Nannochloropsis gaditana* revealed the identification of four TPT genes. Only one of these genes exhibits significant homology with Apicomplexa TPT, sharing conserved features such as 10 membrane-spanning domains and a chloroplast transit peptide, indicating a possible role in DHAP import into the plastid. Instead, the other 3 transporter act importing DHAP into the cytosol. Notably, the down-regulation of these 4 TPT genes in high light conditions suggests a reduction in DHAP import

[44] Alboresi et al.
[45] Ouellette and Rawn, *Organic Chemistry*.

into the chloroplast, promoting fatty acid biosynthesis in the cytosol and endoplasmic reticulum. This supports the hypothesis that TPT translocators play a role in regulating metabolic fluxes in *N. gaditana*[46].

In phototrophic organisms, including *Nannochloropsis spp*., all reduced carbon molecules are initially synthesized in the chloroplast and can be either directly utilized or exported to the cytosol. Adaptation to high light involves a significant reorganization of organelle roles, supporting a scenario where reduced carbon molecules can be transported back to the chloroplast to fuel plastid biosynthetic pathways. This suggests a regulatory loop for carbon partitioning between the chloroplast and cytosol, modulated by specific transporters. The regulation of metabolite fluxes in and out of the chloroplast emerges as a major mechanism in the metabolic remodeling of the entire cell (Figure 12). This regulation, coupled with *N. gaditana* unique ability to synthesize fatty acids in the cytosol, enables sustained lipid biosynthesis in the endoplasmic reticulum even under stress conditions[47].

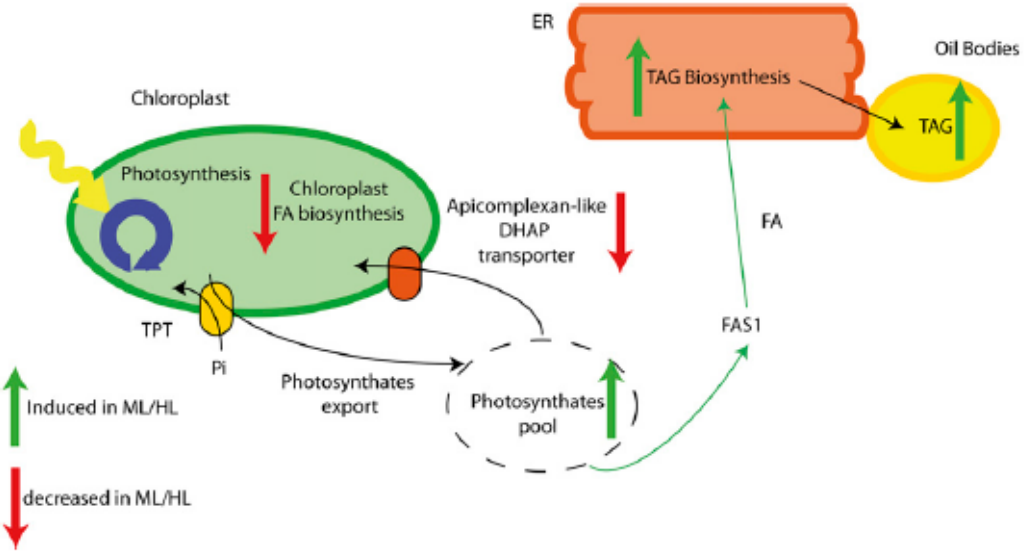

FIGURE 12: Model of regulation of carbon partitioning and lipid metabolisms in *N. gaditana* cells[47].

[46] Alboresi et al., 'Light Remodels Lipid Biosynthesis in *Nannochloropsis Gaditana* by Modulating Carbon Partitioning between Organelles'.

A recent study on TPT transporters in the phylogenetically distant organism *Chlamydomonas reinhardtii*[47] (Figure 13) reveals that mutants incapable of producing this transporter exhibited light sensitivity, severe growth impairment, and substantial changes in their metabolic profiles compared to unmutated cells. This implies that the absence of this transporter has a substantial impact on the organism's ability to carry out essential metabolic processes and suggest that the transporter may play a vital role in protecting Chlamydomonas from the harmful effects of excessive light exposure.

These shifts in cellular metabolism created a toxic intracellular environment characterized by reactive oxygen species (ROS) production, implying that *Chlamydomonas* cannot compensate for the loss of TPT through the activities of other transporters[48].

So, in *C. reinhardtii*, TPT serves as a major conduit at the chloroplast envelope for the trafficking of fixed carbon, supporting various vital cellular functions such as central carbon metabolism, energy dissipation, efficient photosynthetic electron transport, prevention of intracellular hydrogen peroxide accumulation, and maintenance of redox balance at the subcellular level. All these findings, suggests the importance of a more in-depth investigation into the functioning of these transporters because understanding the diverse functioning of TPT across organisms can provide insights into exploitation or modification possibilities.

[47] Huang et al., '*Chlamydomonas* Mutants Lacking Chloroplast TRIOSE PHOSPHATE TRANSPORTER3 Are Metabolically Compromised and Light Sensitive'.

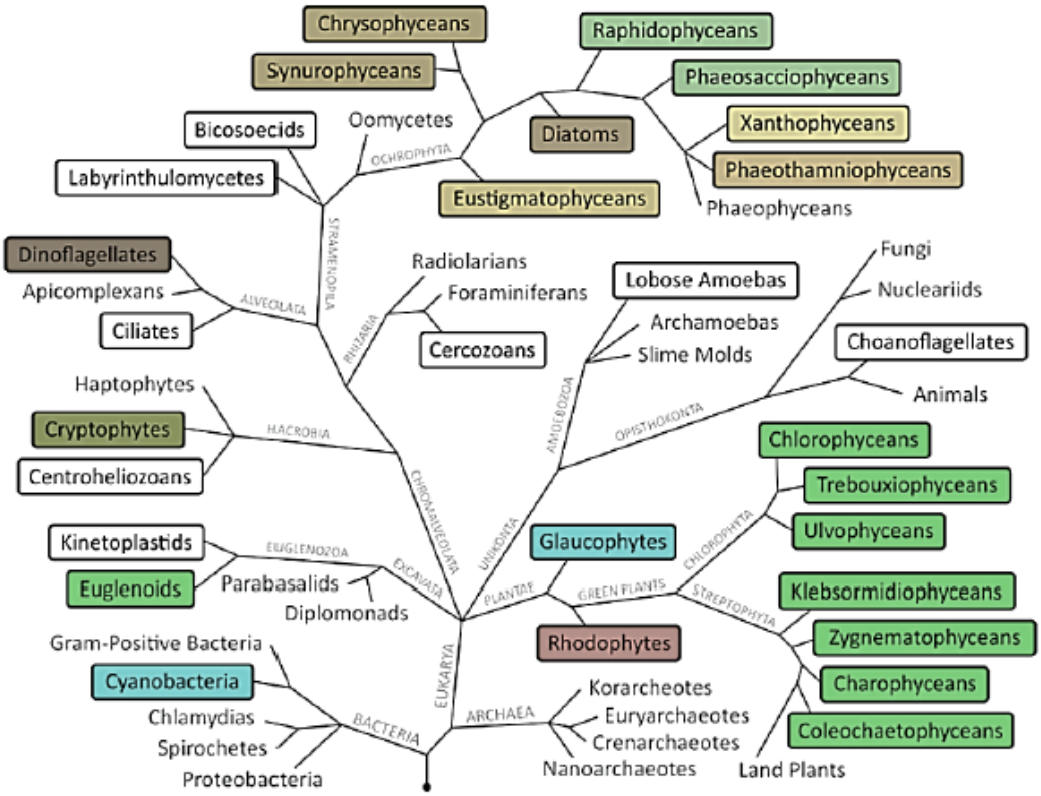

FIGURE 13: Phylogenetic tree representing the relations between microalgae classes. Species of *Nannochloropsis* are in the class of Eustigmatophyceans, while *Chlamydomonas* are in the class of Chlorophyceans. Figure adapted from (http://www.keweenawalgae.mtu.edu)

2. Aim of the thesis

The food industry is currently facing the challenge of achieving a significant higher productivity, both in terms of animal and plant-based derivatives. The increasing global demand for food is placing immense pressure on our ability to produce enough food. Furthermore, this extensive food production is significantly affecting the environment, contributing to greenhouse gas emissions, habitat loss and the excessive use of energy, freshwater and fertilizers.

In recent years, microalgae have emerged as promising microorganisms with diverse applications, offering a wide range of valuable products and a sustainable alternative for food production, due to their biomass composition, high photosynthetic rate and ability to grow on different substrates without consuming arable land. Microalgae do not compete with plants for arable land because they thrive without the need for fertile soils. This characteristic allows for the exploitation of marginal and non-productive areas, such as deserts. Also, their unique ability to proliferate in diverse aquatic environments, including seawater or even wastewater, makes them well-suited for cultivation in areas where traditional agriculture is challenging and playing a crucial role in bioremediation which makes their production even more sustainable by reducing the demand for energy, fertilizers and water.

Microalgae can provide proteins, carbohydrates, lipids, and various pigments with antioxidant, anti-inflammatory, and dye properties. They also surpass terrestrial crops in their ability to yield diverse bioactive compounds, offering health and nutritional benefits.

Nannochloropsis, in particular, has garnered considerable attention due to its capacity to accumulate a substantial fraction of reduced carbon as lipids, which play a crucial role in the human diet. Long-chain polyunsaturated fatty acids (PUFAs) are especially important for human nutrition and are largely absent in oils derived from terrestrial plants. These bioactive substances, confer anti-inflammatory activity and positive health effects.

Essential fatty acids, like ω-3 and ω-6, are not naturally produced by humans but can be incorporated into the diet. For instance, they are found in fish, which obtain them by consuming marine algae, the primary producers of these substances. Therefore, studying and understanding the mechanisms that regulate carbon fluxes within the cell and the lipid biosynthesis pathway is crucial to harness the full potential of microalgae.

This thesis focuses on two distinct aspects of lipid metabolism. In the case of *Nannochloropsis gaditana*, we utilized KO mutants of the Apicomplexan-like DHAP transporter (referred to as TPT transporter from now on), obtained through CRISPR-Cas technology with two goals:

- understand the role of this transporter in the cell carbon partitioning, cell growth and lipid metabolism
- test if the mutants were able to accumulate photosynthates and increase the production of lipids in the cytosol in low light conditions

In our case this light condition is essential because in low light (LL) than to medium light (ML) and high light (HL), DHAP is more abundant than others carbon intermediate and it is an essential molecule in the metabolism, being an intermediate in various metabolic pathways.

Given the putative function of the targeted TPT gene, in the analysed mutants the reduce carbon molecule transport back to the chloroplast was expected to be blocked (or reduced). The desired mutation was confirmed through PCR in five independent *N. gaditana* mutants. To assess their growth and neutral lipid production, we conducted some growth curves coupled to Nile red staining measurements.

For *Nannochloropsis oceanica*, our aim was to overexpress a specific desaturase to understand its function and improve the fatty acids profile. We used a *Nannochloropsis oceanica* tdTOMATO strain (IMET1) gifted by Sarah D'Adamo (Wageningen University) optimized for genes insertion (HR), over-expression and rapid mutants selection (Sudfeld et al., 2021). The target desaturase of this work is putatively involved in converting ω-6 fatty acids to ω-3 fatty acids, specifically the conversion of arachidonic acid

(C20:4, n-6, ARA, ∆5,8,11,14) to eicosapentaenoic acid (C20:5, n-3, EPA, ∆5,8,11,14,17) (Figure 14). The ultimate goal is to improve the ω3/ω6 ratio of the lipid profile, enhancing its nutritional value and health benefits.

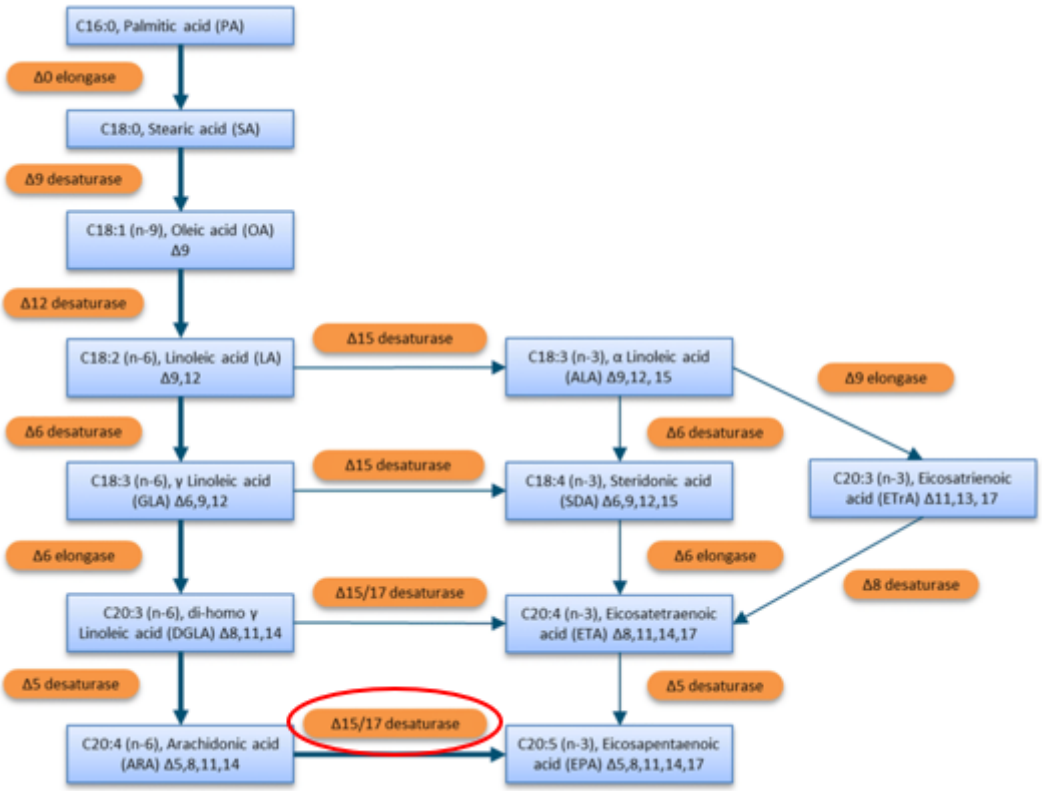

FIGURE 14: General proposed PUFA biosynthesis pathway for *Nannochloropsis*[48]. Our putative desaturase is the red circle one and it is involved in converting ω6 fatty acids into ω3 fatty acid, catalyzing the transformation of Arachidonic acid into Eicosapentaenoic acid

This transformation is part of a broader project, aimed at optimizing microalgae lipid metabolism for the sustainable production of edible oils. The primary objective is to develop a valuable alternative to palm oil, as creating a microalgae-derived substitute holds significant promise for mitigating the environmental impacts associated with intensive palm cultivation.

[48] Janssen et al., 'Time-Dependent Transcriptome Profile of Genes Involved in Triacylglycerol (TAG) and Polyunsaturated Fatty Acid Synthesis in Nannochloropsis Gaditana during Nitrogen Starvation'.

3. Material and methods

3.1 *Nannochloropsis* culture

Nannochloropsis gaditana wild type from CCAP (Culture Collection of Algae and Protozoa), strain 849/5 and *Nannochloropsis oceanica* tdTOMATO strain (IMET1) gifted by Sarah D'Adamo (Wageningen University) were used for our experiments. Media for *Nannochloropsis* spp. cultivation were prepared using sterile f/2 medium (Guillard and Ryther, 1962), containing 32 g/L Sea salts (S9883; Sigma-Aldrich), 40 mM Tris-HCl, pH 8, and Guillard's (f/2) marine water enrichment solution (G9903; Sigma-Aldrich). To obtain PLUS medium NaH_2PO_4 and $NaNO_3$ were added to the final concentrations of 0.042 mM and 8.82 mM, respectively, together with vitamin mix, trace metals, Na_2 EDTA, and $FeCl_2$. Cultures were generally kept in shaking autoclaved 250 mL flasks under continuous light at 100 µmol photons m^{-2} s^{-1} and refreshed 1-3 times per week to avoid nutrient limitation. For maintenance or after transformation, microalgae were kept on Petri plates with the same f/2 medium supplemented with 10 g/L of Plant Cell Tested Agar. In Petri plates there is the possibilities to use a selective medium, by adding antibiotics to find a mutant after a transformation or to remove bacterial contamination. Generally, cultures on agar plates should be transferred onto fresh solid medium once a month.

All microalgae were maintained at a temperature of 22 ± 1°C.

3.2 *N. gaditana* physiological analyses

For the **growth curves experiments**, *N. gaditana* strains were pre-inoculated in flasks with 50 mL of PLUS shaking, under 50 µmol photons $m^{-2}s^{-1}$ of light intensity, atmospheric CO_2 and 22 ± 2°C temperature. In order to keep the algae in exponential growth phase and reduce the pre-inoculum variability, cells were diluted twice (every 3-4 days) to OD750 = 0.2 before starting the experiment.

At the end of the pre-inoculum phase, this culture was pelleted and used to start the growth curve on 6-well plates with f/2 medium at the constant

temperature of 21°C, 1% of CO_2, under 40 µmol photons $m^{-2}s^{-1}$ for 7 days. The volume for each well was 4 mL, with a starting OD750 ~ 0.2, corresponding to about 20 x 10^6 cells/mL (Figure 15).

OD750 and the cell concentration were measured at day 0, 3, 4, 5, 7. The neutral lipid content was determined by staining the algal cell suspensions with Nile red dye and measuring the resulting fluorescence with two different instrument, a fluorescence spectrophotometer Cary Eclipse (Agilent Technologies) or a *Spark multimode microplate reader* (TECAN) spectrofluorometer with a 96-well dark plate.

PSII maximum efficiency expressed as Fv/Fm = (Fm-F0)/Fm was monitored through in vivo chlorophyll fluorescence determination with the DUAL-PAM-100 fluorimeter (Heinz-Walz) at day 0 and 7 to assess the viability of the cells.

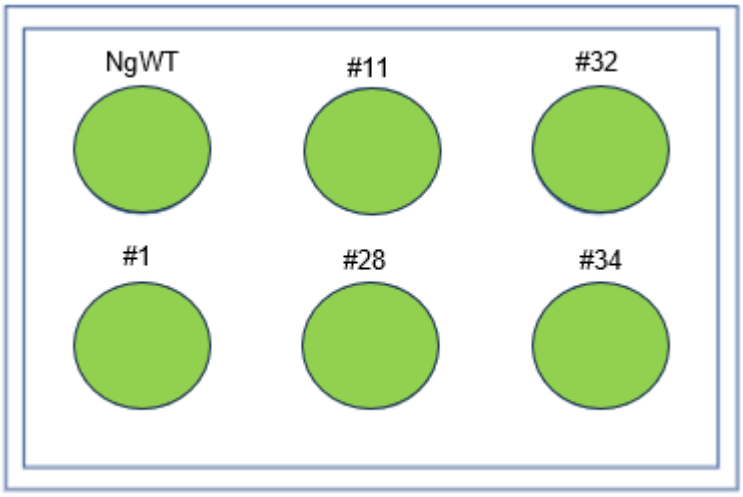

FIGURE 15: plate 6-line disposition

3.2.1 *N. gaditana* spot test

To carry out a preliminary growth characterization, spot tests on plates with different light intensity and cell concentrations were prepared. Were tested 3 different growth concentration:

- $10*10^6$ cells (1:1)
- $1*10^6$ cells(1:10)

- $1*10^5$ cells(1:100)

And 2 different light intensity:

- Low Light: 70 µmol photons $m^{-2}s^{-1}$
- High Light: 900 µmol photons $m^{-2}s^{-1}$

For each plates 12 spots were made. Plates were prepared as indicated in Figure 16 (2 biological replicates for each different light intensity).

From each line of *N. gaditana* liquid cultures were prepared three serial 1:10 dilutions and 40 µL of each were deposited in one area of the plate. Spots were left dry and then the plates were incubated at 22 ± 2 °C. Plates were controlled in day 0, 3 and 7.

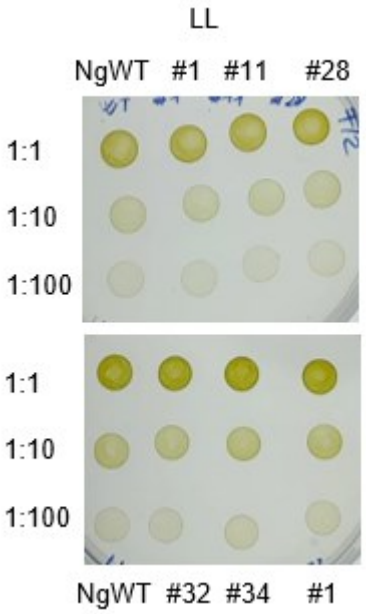

FIGURE 16: Distribution of each strain in the spot test. WT must be present in each plate to act as control. Every plate has a biological replicate in the same condition of light intensity. 1:1 = $10*10^6$ cells; 1:10 = $1*10^6$ cells; 1:100 = $1*10^5$ cells

3.2.2 OD and cell count

The Optical Density (OD) measurement were obtained through the use of the *Spark multimode microplate reader* (TECAN) spectrofluorometer at 750 nm, using 200 µL of the sample in a 96-well plate. The sample was eventually diluted to remain in the linear range (OD750 between 0.1 and 1.0) of the instrument.

To count the number of cells per millilitre of culture, a Cellometer Auto X4 from Nexcellom bioscience was used. This instrument is able to count cells within slides in which 20 µL of culture are loaded on counting chambers. After loading, we waited 10 minutes for the cells to settle on the bottom and be focused on the same plane. The instrument returns the cell concentration in bright field and in fluorescence, to discriminate the total population of cells

and just the population of cells alive. The instrument also reports the average diameter of cells.

3.2.3 Neutral lipid measurements

Neutral lipid content was analyzed using Nile red dye (NR: 9-Diethylamino-5H-benzo[α]phenoxazin-5-one, SIGMA). It is a non-polar fluorophore that co-localizes with neutral lipids and, when excited at the appropriate wavelength, emits fluorescence in a range between 575 and 585 nm.

The NR solution was prepared at a concentration of 0.5 mg/mL in acetone and stocked at -20°C protected from light.

For the cells staining, two different protocols were used:

- For the fluorescence spectrophotometer Cary Eclipse (Agilent Technologies) were prepared for each sample 20 x 10^6 cells that were stained with 2,6 µg/mL (10 µl of stock) of NR in 1.9 mL of deionized water. Cells were incubated shaking for 20 minutes at 37°C in the dark. Excitation wavelength was set at 488 nm and fluorescence emission was acquired between 500 and 750 nm to include both the signal from Nile Red and chlorophylls. The average of intensity values (A.U.) in the range 560-610 nm (i.e. the maximum NR fluorescence region) was used as an estimate of the neutral lipids amount in the sample
- For the TECAN were prepared for each sample 2 x 10^6 cells that were stained with 2,6 µg/mL (1 µL of stock) of NR in 200 µL of deionized water. Cells were incubated shaking for 20 minutes at 37°C in the dark. The fluorescence was measured exciting the fluorophore at the wavelength of 485 nm and collecting the emission value at 585 nm. In this case, the gain value was maintained constant, to compare measurements between different days of the growth curve.

In both cases, the same number of unstained cells were analyzed as a control to eliminate the fluorescence signal given by the cell culture. The

relative fluorescence of Nile red for the neutral lipids quantification was obtained from the subtraction of the autofluorescence of algal cells and Nile red alone.

Finally, since Nile red is a light-sensitive dye, in all the phases of the measurements, samples with the staining (and the dye itself) must be kept in the dark as much as possible. So a black 96-well plate (SARSTEDT) was used to perform the measurements at TECAN also because the transparent 96-well plate reflects light in a fluorescence measurement that can give problems.

3.2.4 Pulse Amplitude Modulation (PAM)

The value of the photosynthetic efficiency (Fv/Fm) of the PhotoSystem II (PSII) was measured *in vivo* through the fluorimeter DUAL-PAM –100 (Walz).

From each sample 1 mL of culture was aliquoted and dark-adapted for 30 minutes at room temperature. The dark adaptation allows all PhotoSystemII (PSII) reaction centers to become open, thus the maximal photochemical quenching can be registered. The Fv/Fm value was measured at the instrument and calculated with the formula:

$$\frac{F_v}{F_m} = (F_m - F_0)/F_m$$

F_v is the variable fluorescence and is given by the difference between the F_m, the maximum fluorescence, and F_0, the minimum fluorescence.

In the dark-adapted state, the minimum fluorescence F_0 value is measured with the 'measuring light', a weak light source used to measure the chlorophyll fluorescence emission of PSII when the photochemical mechanism has the maximum efficiency.

In this condition, PSII centers are open and no NPQ is present, the photochemistry efficiency is maximum and most of the excitation energy, coming from the measuring light, is exploited by this mechanism

(photochemical quenching). The fraction of the energy that is not used is re-emitted as fluorescence and measured by the instrument.

In stress conditions, the photochemical quenching efficiency is reduced and the energy dissipates as fluorescence increases and consequently the F_0, value that is measured (reducing the F_v value and the F_v /$F_m$ratio).

From the application of a high-intensity saturating pulse, all the reaction centers of PSII close, and the photochemical quenching is saturated. In this condition, is measured the maximum value of energy dissipated as fluorescence by the PSII chlorophyll, F_m. It is considered just the photosynthetic efficiency of the PSII since the fluorescence emitted from the PSI is negligible compared to it.

3.3 Molecular biology

3.3.1 RNA extraction

To perform RNA extraction, about 250 million cells was pelleted at 12000 x g for 10 minutes at RT; after removing the supernatant, a volume of 50 µL of TRizol reagent (Invitrogen) and 150-200 µm glass beads were added to cover the pellets, then the samples were subjected to 3 rupture cycles at the Bead-Beater (Biospec.) or Tyssue Lizer for 20 seconds at maximum speed, interspersed with 1 minute at RT.

An additional 950 µl of TRizol werethen added and a new 20-second cycle of Bead-Beater or Tyssue Lizer were performed at maximum speed. and the sample were swirled via vortex for 15 seconds to promote the dissociation of the multiprotein complexes.

After 5 minutes of rest at RT, 200 µL of chloroform were added and the sample were stirred via the vortex for 10 seconds and rest for another 10 minutes at RT. At this point, the samples were centrifugated at 4°C for 10 minutes at 12000 x g and this allowed to distinguish 3 phases:

- An upper, colorless aqueous phase containing RNA
- An intermediate stage containing DNA

- A red-colored organic phase on the bottom of the tube.

The upper phase was recovered and placed in another tube, where 500 µL of isopropanol for mL of TRIzol used were added. After 10 minutes, the samples were centrifuged again at 4°C, for 10 minutes at 12000 xg. This centrifugation allows the RNA to precipitate to the bottom of the tube, where it will form a white-colored pellet. At this point the supernatant were removed, and the RNA pellet were washed by adding 1 mL of EtOH 75% for mL of TRIzol used.

After this the sample were swirled with vortex and then were centrifugate at 4°C for 5 minutes at 12000 x g. The wash cycle was repeated another time with 500 mL of EtOH 75%

At this point, the supernatant was removed and the pellet was left to dry for 15 minutes under the hood. Finally, pellet was resuspended in 30 µL of sterile H_2O, to allow it to dissolve. If the pellet struggles to resuspend, the following procedure can be followed:

- 15 seconds of vortex
- 5 minutes at 65°C
- 15 seconds of vortex

Concentrations were quantified by evaluating the 260/280 and 260/230 ratios (they must be at least 1.8).

3.3.2 DNaseI treatment

To eliminate DNA contamination, starting from a 1 µg sample of RNA (quantification by the NanoDrop ND-1000 spectrophotometer - CelBio), a deoxyribonuclease (DNase) treatment were performed by adding to the RNA:

- 1 µL 10X *reaction* buffer with MgCl2
- 1 µl DNase I, *RNase*-free 1 U – Thermo scientific
- H_2O up to a total volume of 10 µl

The reaction mix were incubated for 30 minutes at RT. 1 µl of *stop* solution were added and the sample were placed at 65°C for 10 minutes. Finally, the tube was placed on ice.

3.3.3 Retrotranscription

The RNA obtained after DNase treatment were used as a template for reverse transcription to obtain cDNA. 1 µl of oligo-d(T), short oligo-deoxyribonucleotides (Thermo scientific) that will pair up in random regions of the template transcripts, were added to the template; then, is the samples were incubated at 65°C for 5 minutes to destroy the secondary RNA structures and then were placed on ice.

Finally, the Thermo scientific kit were use, adding to the tube:

1. 4 µl RT reaction buffer
2. 0.5 µl RT Ribolock (RNase inhibitor)
3. 2 µl dNTPs (10 mM)
4. 1 µl Reverse Transcriptase

The samples were incubated for 1 h at 42°C and then were stored at 4°C.

3.3.4 Genomic DNA extraction

Chelex-100 resin (Bio-Rad) was used to extract genomic DNA from N. oceanica colonies growing on solid medium. 200 µl of 5% (m/v) Chelex-100 solution in sterile water were placed in a PCR tube and a small amount of algal sample was taken from the solid medium. After resuspension in Chelex-100 solution, the samples were heated at 95°C for 20 minutes and then kept at 4°C for 20 minutes. After vortexing for one minute, the samples were centrifuged at 14000 xg for 3 min to pellet the resin and the cellular debris. The transparent supernatant then contained the genomic DNA.

3.3.5 Polymerase chain reaction (PCR)

PCR reaction allows the amplification of DNA regions of interest from DNA sources. It can be used qualitatively for screenings or to amplify a DNA sequence. Were used two different types of polymerases:

1. Dream Taq Green PCR Polymerase Master Mix (2x) (ThermoFisher) which has a throughput of 1000 bp/minute (Table 1)
2. Platinum Superfi II DNA Polymerase Master Mix (2X) (Thermofisher) which has a throughput of 2000 bp/minute (Table 2)

The reaction cycle was shown in the table:

	Temperature [°C]	Time [min:sec]	
Initial denaturation	95	5:00	
Denaturation	95	0:30	X 35 cycles
Annealing	Tm	0:30	
Extension	72	60 s/kbp	
Final extension	72	5:00	
Conservation	16	Infinity	

TABLE 1: Reaction cycle used in amplifications with the Dream Taq Green PCR Polymerase (Thermofisher) Tm=annealing temperature of the primer

	Temperature [°C]	Time [min:sec]	
Initial denaturation	98	0:30	
Denaturation	98	0:10	X 35 cycles
Annealing	Tm	0:10	
Extension	72	30 s/kbp	
Final extension	72	5:00	
Conservation	4	Infinity	

TABLE 2: Reaction cycle used in amplifications with the Platinum Superfi II DNA Polymerase (Thermofisher) Tm=annealing temperature of the primer

The PCR reactions composition were shown in the table were composed of: 1 µl of Chelex of each transformant colony as DNA template, using the tdTOM strain as control, 0.2 mM of each primer (pCpTE seq-for and pCpTE

seq-rev), 10 µl Platinum SuperFi II DNA Polymerase master mix (Invitrogen) in a total volume of 20 µl. Amplification of inserted gene constructs was analysed by agarose gel electrophoresis.

PCR reactions were composed of 1 µl of Chelex from each line to control as a DNA matrix, using wild-type as a positive control. Primers, polymerase and sterile H2O by volume are added to the reaction mix.

Master Mix	Volume (µL)
PFW	0,5
PRV	0,5
DNA Polymerase (2X)	5
H_2O	3
DNA/Template	1 ≈ 10 ng
Vol. tot	10

TABLE 3: general volume for a PCR reaction

3.3.6 Agarose gel electrophoresis

This technique was used to verify that PCR-amplified fragments are of the expected length, separating PCR products on the basis of their molecular weight.

To obtain a 1% agarose gel, the agarose (SIGMA) was dissolved in a TAE buffer (40mM Tris pH 8, 20mM acetic acid, 1mM EDTA), then the EuroSafe nucleic acid stain (Euroclone) 20,000X was added to a final concentration of 1x. The gel obtained was then solidified and placed in a tray containing TAE 1X. Samples were loaded into wells, and a molecular weight marker, the GeneRuler 1 kb DNA Ladder (Thermofisher) (Figure 17), was also loaded to verify the difference between molecular weights. To separate the DNA fragments, an electric field was used under conditions of constant voltage (100 or 110 V) for 15-30 minutes.

To observe the result of the migration at the end of the run, the gel was analyzed by placing it on a UV transilluminator.

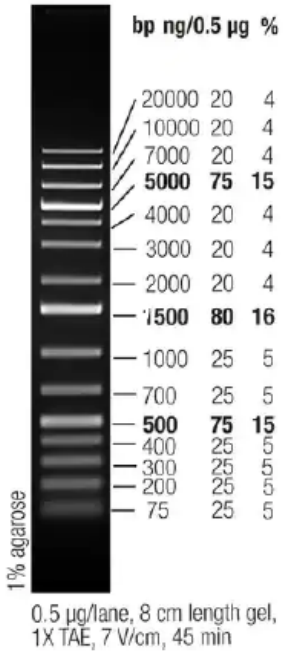

FIGURE 17: GeneRuler 1 KB DNA Ladder (Thermofisher) molecular weight marker with band associated to DNA concentrations

3.3.7 *E. coli* DH5α competent cells heat-shock transformation

In order to prepare, purify and obtain the plasmid to carry out the transformation, a heat-shock transformation of *E. coli* competent cells was performed. 5 µL of ligation between plasmid and DNA were added to 50 µL of competent DH5α cells that before were thawed on ice for 5 min. After incubation for 20 min, a heat shock of 45 s at 42°C was performed and the cells were placed on ice for 2 min. Subsequently, 500 µL of LB were added and the cells were grown at 37°C for 1 h under shaking. Then the cells were pelleted for 2 minutes at 12000 x g, 400 µL of the surnatant were removed and the cells were gently resuspended in the remaining volume. Finally, the bacterial culture was plated onto LB + Amp and grown overnight at 37°C.

E. coli cells were cultured at 37°C in liquid LB medium (Table 4) under shaking or plated on solid LB medium. Ampicillin at a concentration of 100 µg/mL was added to obtain selective media (LB+Amp).

Component	Concentration
Yeast extract	5 g/L
Tryptone	10 g/L
NaCl	10 g/L
Agar (for solid medium)	15 g/L

TABLE 4: LB medium composition

3.3.8 Colony PCR

For *E. coli* DH5α transformant colony screening a slightly different PCR protocol was used, called Colony PCR. Each colony to screen was picked and diluted in 50 µL of deionized water. Then 9 µL of each colony dilution were added to the PCR mixture as DNA template together with the OrangeTaq mix and pCpTE seq-for and pCpTE seq-rev primers (Table 5, Table 10). The initial denaturation step at 95 °C was prolonged up to 10 min to allow bacterial cells to lysis and release their plasmid in the reaction (Table 6). Finally, the size of the amplified fragments were analyzed by agarose gel electrophoresis and purified with the PCR purification kit (Thermo Scientific). Correct insertion and orientation of the insert was confirmed by sequencing.

OrangeTaq mix was prepared in our lab and it contains: Taq polymerase enzyme, buffer with dNTPs and the Orange G loading dye.

Component	Volume (µL)
OrangeTaq mix	10
Bacterial suspension	9
PFW	0,5
PRV	0,5

TABLE 5: Reaction mix for the colony PCR

	Temperature [°C]	Time [min:sec]	
Initial denaturation	95	10:00	
Denaturation	95	0:30	X 35 cycles
Annealing	57	0:20	
Extension	72	1:45	
Final extension	72	4:00	

TABLE 6: PCR program for colony PCR to confirm the presence of the insert FADw3 in the plasmid pCpTE

3.3.9 Plasmid DNA extraction from bacterial cells

To purify plasmid DNA from bacteria, the cells were cultured overnight in 5 mL of LB liquid medium with ampicillin and a pellet was obtained by a centrifugation step at 14000 xg for 3 minutes. Plasmid DNA was extracted using the GeneJet Plasmid Miniprep kit (ThermoFisher).

To obtain a larger amount of DNA, the bacterial cells with the desired plasmid were cultured overnight in 50 mL or 100 mL of LB + Amp. After the cells were centrifuged at 5000 xg for 5 min, the GeneJet Plasmid Midiprep kit was used (ThermoFisher) to obtain plasmid DNA. Final plasmid concentrations were measured with NanoDrop (ND-1000 spectrophotometer, CellBio).

3.3.10 Cloning strategy

Südfeld et al. (2021)[49], developed and optimized a novel gene expression system in the microalga *Nannochloropsis oceanica* that confers exceptionally high gene expression by recruiting the cellular rRNA synthesis machinery for transcription. They identified the nucleolus as a genomic safe harbor for polymerase I transcription and used it to construct transformant strains with consistently strong transgene expression. In the same work, they used the newly discovered information to construct a ‘‘landing pad’’

[49] Südfeld et al., ‘The Nucleolus as a Genomic Safe Harbor for Strong Gene Expression in Nannochloropsis Oceanica’.

(LP) strain (LP-tdTomato) that expresses the fluorophore tdTOMATO. When this strain, (from now on called tdTOM) is transformed with a DNA construct presenting flanks that are homologous to the LP, it can be integrated and a loss of fluorescence occurs as the result of the replacement of the tdTOMATO cassette. Following this new system, not only high expression levels are permitted, but also an easy high-throughput screening method is feasible.

In order to generate FADω3 overexpression (OE) strains, the construct used to transform the tdTOMATO strain were obtained by inserting the gene of interest FADω3 into the pCpTE vector[50], which contained the homology regions for recombination, the necessary elements translation, and a Blasticidin resistance cassette (Figure 18).

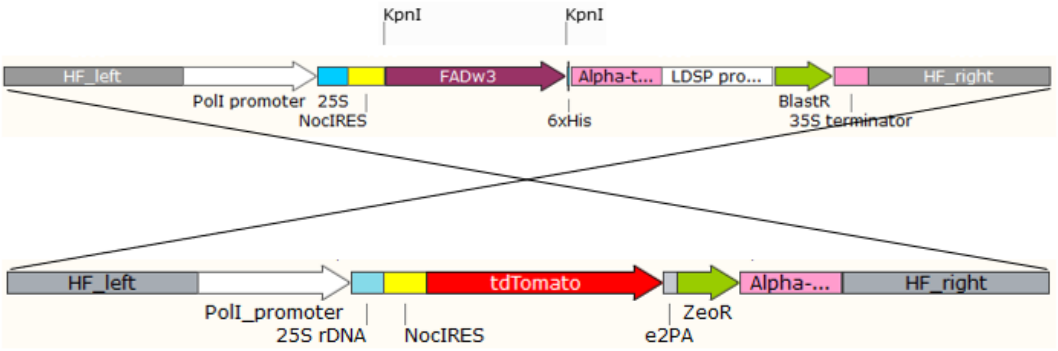

FIGURE 18: Graphic scheme of the gene constructs FADω3 used to transform the N. oceanica tdTOM strain. PolI prom = polymerase I translation promoter; 25S = 25S rDNA fragment; NocIRES = internal ribosome entry site of N. oceanica; FADω3 = coding sequence of fatty acid desature; 6xHis = tag of 6 Histidine used in affinity column purification; α-tub ter = α-tubulin terminator; LDSP Prom = promoter of the lipid droplet surface protein; BlastR = gene coding for the resistance to Blasticidin; 35S ter = translation terminator of 35S gene; HF =homologous region; tdTOMATO = gene for fluorophore tdTOMATO. ZeoR = gene coding for the resistance to Zeocin; KpnI restriction sites used in the cloning strategy are indicated with a small black line.

The FADω3 coding sequence was amplified from cDNA with Platinum Superfi II DNA Polymerase (Thermofisher) and the primer NoFADω3_fw and NoFADω3_rv. The DNA was purified with the PCR purification kit and then was used to make another PCR with the primer overhang to introduce

[50] Südfeld et al.

the sequence of the restriction enzyme KpnI on the sides of the coding sequence (Table 8). The PCR was purified with the PCR purification kit (Thermo scientific) and the obtained FADω3 construct was eluted in 30 µL of water. 14 µL of the eluted DNA were digested with 2 µL of KpnI, 3 µL of Buffer and 11 µL of H_2O for 2.5 h at 37°C. The digestion buffer and the KpnI enzyme was subsequently removed by purifying the construct again with the PCR purification kit.

The cloning strategy involves the use of pCpTE-KpnI plasmid linearized with dephosphorylated ends. 10 µg of pCpTE-KpnI plasmid were digested with 1 µL KpnI enzyme in KpnI buffer for two hours at 37°C in a total volume of 20 µL. To remove the digestion buffer and KpnI, a PCR purification step was performed and the digested ends were dephosphorylated in order to avoid plasmid religation. For this reaction, the restricted plasmid was incubated with 1 µL of Antarctic phosphatase (New England Biolabs, M0289S) in phosphatase buffer (New England Biolabs, B0289S) for one hour a 37°C in a total volume of 35 µL. After another PCR purification step eliminating the phosphatase, it was possible to proceed with the ligation of pCpTE with the FADω3 construct.

For ligation of the pCpTE plasmid with the FADω3 insert, different ratios between the plasmid and the insert were mixed as illustrated in table 7. The ligation reaction was performed at 16°C overnight

Reaction Mix	Ctrl (µL)	2:1 (µL)	3:1 (µL)	5:1 (µL)
FADω3	-	0,2	0,3	0,5
pCpTE-pol_KpnI	0,5	0,5	0,5	0,5
T4 Ligase (NEB)	0,5	0,5	0,5	0,5
Ligase Buffer (10x)	2	2	2	2
H_2O	17	16,8	16,7	16,5
TOT volume (µL)	20	20	20	20

TABLE 7: Components and ratios used for the ligation of the plasmid pCpTE and the insert FADω3

The day after, *E. coli* DH5α cells were transformed with pCpTE ligated with FADω3, and a colony PCR was performed. The size of the amplified

fragments was analyzed by agarose gel electrophoresis and correct insertion and orientation of the insert was confirmed by sequencing.

To promote homologous recombination, the exogenous DNA needs to be linear and not in plasmidic form. The linear DNA fragment was obtained by performing a PCR, which permitted the amplification of the entire pCpTE plasmid excluding the Ampicillin resistance cassette and the bacterial open reading frame. The reaction contained 25 ng of pCpTE plasmid, 1 µL dNTPs (Thermo Fisher scientific), 10 µL of 5X Buffer (Thermo Fisher scientific), 1 µL of Phusion DNA pol I (Thermo Fisher scientific), 2,5 µL PFW (oCST033) 2,5 µL PRV (oCST034) in a total volume of 50 µL (Table 10). The linearized fragments were confirmed on agarose gel electrophoresis and purified with the PCR purification kit (Thermo Scientific).

3.4 *N. oceanica* transformation

For the mutagenesis of *N. oceanica* tdTomato strain (IMET1) were used a transformation by electroporation protocol, using the ECM 630 *Electro Cell Manipulator* (BTX ®). Materials overview:

- Recovery medium: F/2 in which the Tris is Plant Cell Tested (SIGMA)
- Selective Plates: Solid F/2 with Agar Plant Cell Tested and Blasticidin
- D-sorbitol Plant Cell Tested 375 mM, pre-cooled to 4°C

N. oceanica tdTOMATO cells for transformation were inoculated in F/2 and cultured in flasks under shaking at 100 µmol photons m^{-2} s^{-1}. When the culture reached the exponential growth phase, it was transferred into a multicultivator to ensure a better air supply and bicarbonate was added at a final concentration of 10 mM. Four days before transformation, the cells were inoculated at an initial concentration of $7x10^6$ cells/mL. For transformation, $500x10^6$ cells/mL were required. The according culture volume was harvested and centrifuged at 5000 xg for 10 min at room temperature. The supernatant was discarded, and the cells were resuspended in 5 mL of D-sorbitol (375 mM), followed by three further centrifuge cycles at 5000 x g for 5 min and washings in D-sorbitol. After the

last wash, the cells were resuspended in a volume of 100 µl D-sorbitol. 2.5 µg DNA was added to the culture volume for each transformation and the samples was put on ice for 10 minutes.

The cell-DNA mix was placed in 2 mm electroporation cuvettes (BTX ®), and electroporated at a voltage of 2400 V (12000 V/cm), a resistance of 500 Ω and a capacitance of 50 µF (using the electroporator ECM 630 Electro Cell Manipulator (BTX). The cells were transferred into 10 mL of recovery medium (F/2 with 40 mM Tris and 40 mM sodium bicarbonate) and grown at low light (20 µmol photons m^{-2} s^{-1}) to allow recovery. After 48 hours, the transformed cells were plated on selective medium containing 100 µg/mL Blasticidin. Resistant colonies appear after 3/4 weeks of exposition at LL (15 µmol photons m^{-2} s^{-1}) in a photoperiod of 12 hours of light and 12 hours of darkness at 22 °C.

4. Results and Discussion

Since the main objectives of this thesis are:

- understand the role of TPT transporter in the cell carbon partitioning and lipid metabolism and how light intensity can modify these
- understand if the mutants were able to accumulate photosynthates and reach a greater production of lipids in the cytosol

As a first step, we started with to the confirmation of the genotype of the mutants by PCR.

4.1 TPT KO mutants genotyping

The *N. gaditana* knockout mutants utilized in this study were generated through CRISPR-Cas technology. To validate the authenticity of the mutants, two distinct PCR analyses (section 3.3.5) were performed, i.e. on genomic DNA and on cDNA. The primers used in these PCRs were designed to bind to the ends of the gene of interest, employing the so called SpeITPT_fw as a forward primer (PFW) and the XbaITPT_rev as a reverse primer (PRV) (Table 10).

Genomic DNA extraction followed the protocol outlined in section 3.3.4, while cDNA was prepared according to the procedures detailed in sections 3.3.1, 3.3.2, and 3.3.3. Subsequently, PCRs resulting products were visualized on a 1% agarose gel (section 3.3.6) under a UV transilluminator and are shown in the next images.

In the PCR on genomic DNA (Figure 19), only the wild-type (WT) sample exhibits a band at the height corresponding to the actual size of the gene (1512 bp). Conversely, the knockout (KO) mutants display bands of larger sizes due to the insertion of an antibiotic resistance cassette, using CRISPR-Cas technology, that disrupts the coding sequence of the target transporter gene. Notably, line 34 exhibits a faint band, albeit at a height consistent with that of the WT.

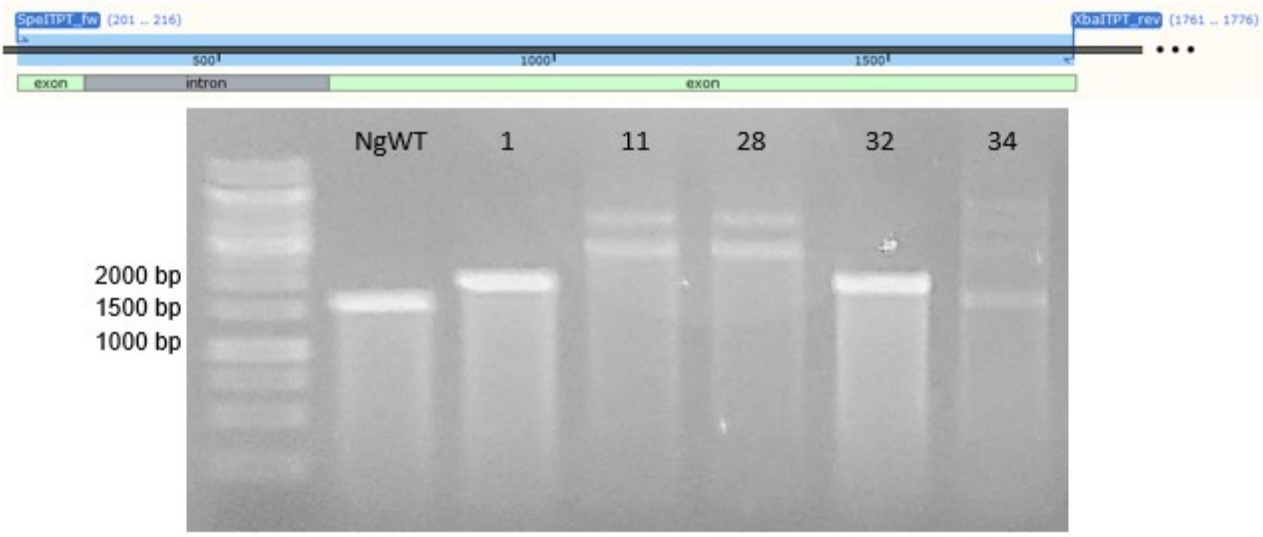

FIGURE 19: genomic DNA PCR and triose phosphate transporter genomic DNA. The expected band for the WT is around 1500 while KO mutants display bands of larger sizes. The map at the top of the image also shows the two primers used and indicated in Table 8

In the PCR on cDNA (Figure 20), an expected band is present only in the WT sample, indicating that the formation of the transcript responsible for transporter production is affected in knockout mutants. The band position, around 1200 bp, accounts for the loss of a 300 bp intron during transcript maturation (map in Figure 19). Notably, the absence of the transporter gene sequence transcription is confirmed also in the mutant 34, confirming successful gene disruption despite the ambiguous PCR results on genomic DNA.

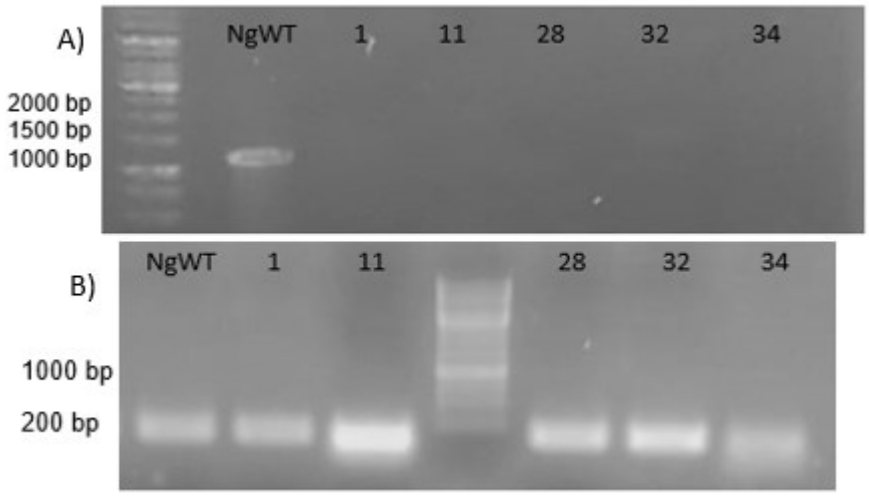

FIGURE 20: A) TPT ko mutants cDNA PCR B) TPT KO mutants qsam PCR. Only WT signal is present. Notably, the absence of the transporter gene sequence transcription is confirmed also in the mutant 34, confirming successful gene disruption despite the ambiguous PCR results on genomic DNA. In the lower part the amplification of the qsam gene, utilized as an endogenous control, is represented.

Finally, in the lower part of Figure 20 the amplification of the qsam gene, utilized as an endogenous control, is represented.

After having successfully genotyped these mutants, these strains were used in growth curve experiments to assess their capacity for neutral lipid accumulation.

4.2 TPT KO mutants growth

First of all, to asses the viability of the cells the F_v/F_m measurement at day 0 has been taken as described in section 3.2.4. The values, that for an optimal viability have to be near 0,6, are indicated in Table 8 and are good to start with the growth curve.

Fv/Fm	
	Day 0
WT	0,583
TPT KO #1	0,574
TPT KO #11	0,570
TPT KO #28	0,576
TPT KO #32	0,577
TPT KO #34	0,568

TABLE 8: F_v/F_m value obtained at DUAL PAM (3 biological replicates). The value obtained are good to start with the growth curve

Secondly, we conducted a 7-day spot test as an initial step in characterizing growth (Section 3.2.1) to investigate whether varying light intensities could influence cellular growth. As depicted in Figure 21, the results after 7 days indicate minimal variation among cells exposed to different light intensities. This lack of significant differences might be attributed to the relatively short duration of the test or the narrow range of disparities in light intensities applied. It's worth considering that a more extended testing period or a

broader range of light intensities could potentially reveal more nuanced effects on cellular growth.

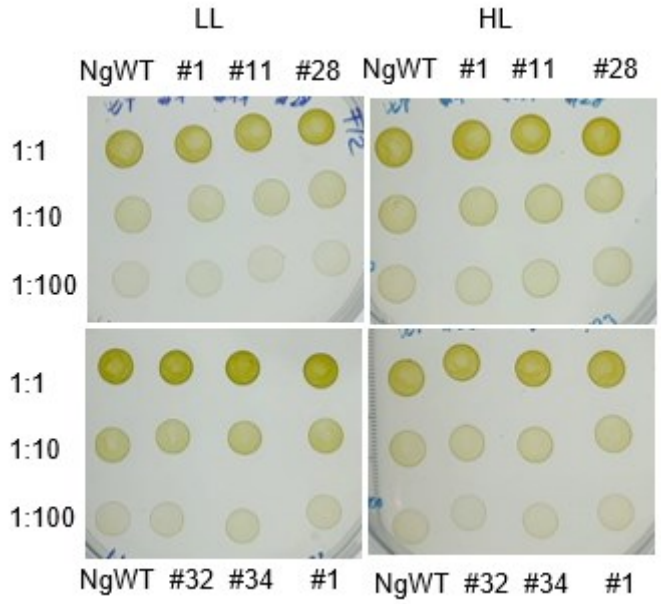

FIGURE 21: Day 7 of the spot test. LL=40 µmol photons $m^{-2}s^{-1}$; HL=400 µmol photons $m^{-2}s^{-1}$; 1:1 = $10*10^6$ cells; 1:10 = $1*10^6$ cells; 1:100 = $1*10^5$ cells. WT line are present in every plate to make comparisons. There doesn't seem to be a difference in the growth

Finally, growth curves were set up following section 3.2. To allow fast preliminary screening of multiple strains under different conditions, each curve was performed using cells distributed across two separate 6-well plates (as depicted in Figure 15). This experimental setup also provided the advantage of having two biological replicates for each cell line. Additionally, to enhance statistical robustness, 2 technical replicates were incorporated in each measurement. The values obtained from these replicates were then averaged to yield reliable results.

Data of the growth curves, presented in Figure 22, indicate that the growth patterns remained consistent and robust throughout the experiment. Both OD measurements and the number of cells per mL suggest that disruption of the transporter does not affect cell growth in mutants respect to the wild type (WT).

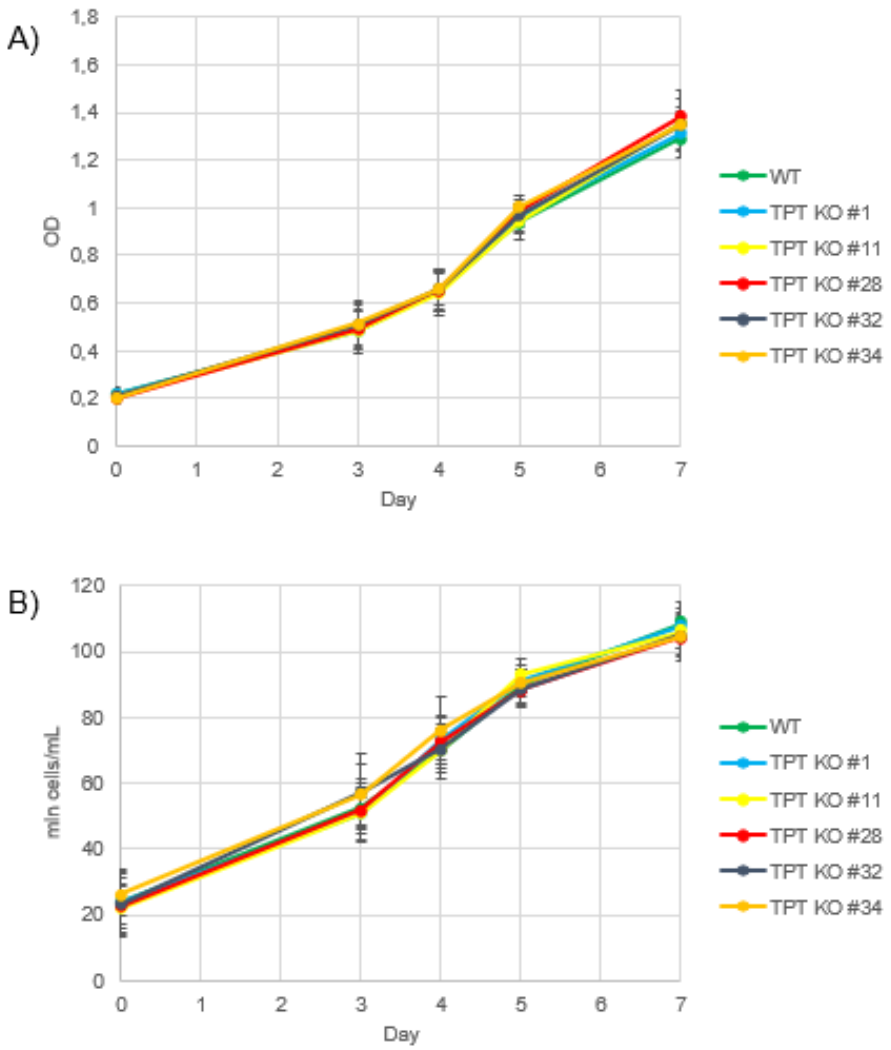

FIGURE 22: Growth measurements obtained in day 0, 3, 4, 5, 7 (6 biological replicates). A) OD measurements obtained at TECAN B) Number of cells per mL obtained at Cellometer. Disruption of the transporter does not affect cell growth and viability in mutants respect to the wild type (WT). Also a reduce in gas exchange due to a reduce in the volume of the well does not affect cell growth

For future investigations, it is advisable to explore experimental parameters such as light intensity, initial cell density, and experiment duration. It's crucial to acknowledge that implementing these modifications might require a larger initial volume. Nevertheless, these adjustments hold the promise of offering more comprehensive insights into the behavior of the knockout mutants, thereby contributing to a more thorough understanding if TPT has an impact on growth in other growing conditions.

4.3 Optimization of Nile red protocol

The assessment of neutral lipid content began with the optimization of the Nile red staining protocol, aiming to standardize the incubation phase to enhance data significance and minimize measurement errors. The optimization process was conducted using a fluorescence spectrophotometer Cary Eclipse (Agilent Technologies) to understand the fluorescence emission spectre of lipid-bound Nile Red. This allowed identifying the precise wavelength at which maximum emission occurs, facilitating subsequent measurements using the TECAN instrument.

The TECAN enabled a larger number of replicates, thereby increasing the statistical reliability of obtained data. Three main parameters were considered during optimization: number of stained cells, Nile red concentration and incubation time. The incubation temperature remained constant at 37°C, based on previous results[51].

First of all, to confirm Nile red binding to cellular lipids, measurements were conducted on WT line subjected to growth in nitrogen-free medium. Under nitrogen-deprived conditions, *N. gaditana* exhibits increased lipid production at the expense of cell growth and other metabolic activities, resulting in a substantial rise in lipid measurements (Figure 23).

To obtain nitrogen-free medium we use the same components of the medium called as PLUS, (Section 3.1) without $NaNO_3$. PLUS medium is used to maintain cells with high nutrient content.

[51] Rumin et al., 'The Use of Fluorescent Nile Red and BODIPY for Lipid Measurement in Microalgae'.

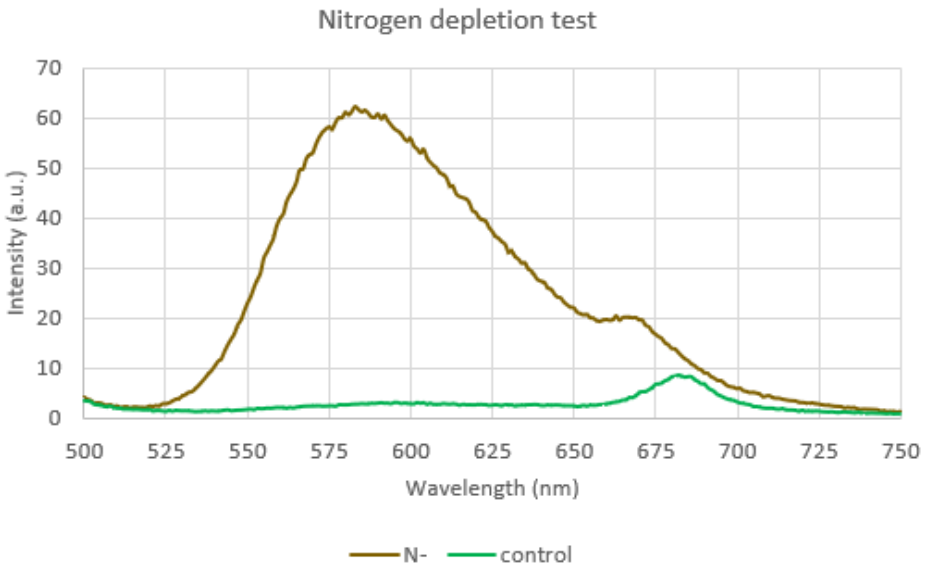

FIGURE 23: Comparison between cells grown without nitrogen (N-, brown one) and cell with control condition (control, green one). Both samples of *N. gaditana* have $10*10^6$ cells and a Nile red concentration of 2,6 µg/mL Under nitrogen-deprived conditions there is a substantial rise in lipid accumulation

With these data, we were also able to verify which was actually the area of the lipid fluorescence peak, i.e. between 560 and 610 nm.

Furthermore, adjusting the amount of Nile red demonstrated an interesting outcome: increased dye quantity led to a reduction in fluorescence (Figure 24). This suggests that an excess of Nile red, due also to the presence of acetone (as dye solvent), have a negative effect on neutral lipid fluorescence, potentially reducing measurement sensitivity.

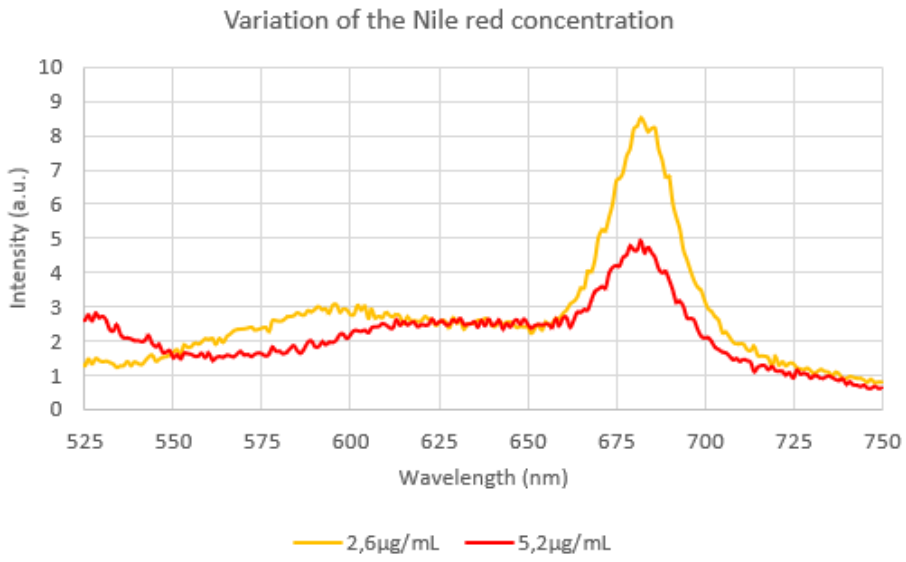

FIGURE 24: Variation of the Nile red concentration. Both samples of *N. gaditana* have $10*10^6$ cells. The orange one have a Nile red concentration of 2,6 µg/mL while the red one have a Nile red concentration of 5,2 µg/mL. Increased dye quantity led to a reduction in chlorophyll fluorescence without proportionally enhancing neutral lipid fluorescence.

At this point, results indicate that the number of cells significantly influences data. Insufficient cells can hamper the acquisition of useful spectra, where the two peaks representing neutral lipids (around 580 nm) and chlorophyll fluorescence (around 680 nm) are clearly distinguishable (Figure 25). So we decided to use 20 millions of cells because in our conditions (i.e with nitrogen) 10 million cells are not enough to have a good signal.

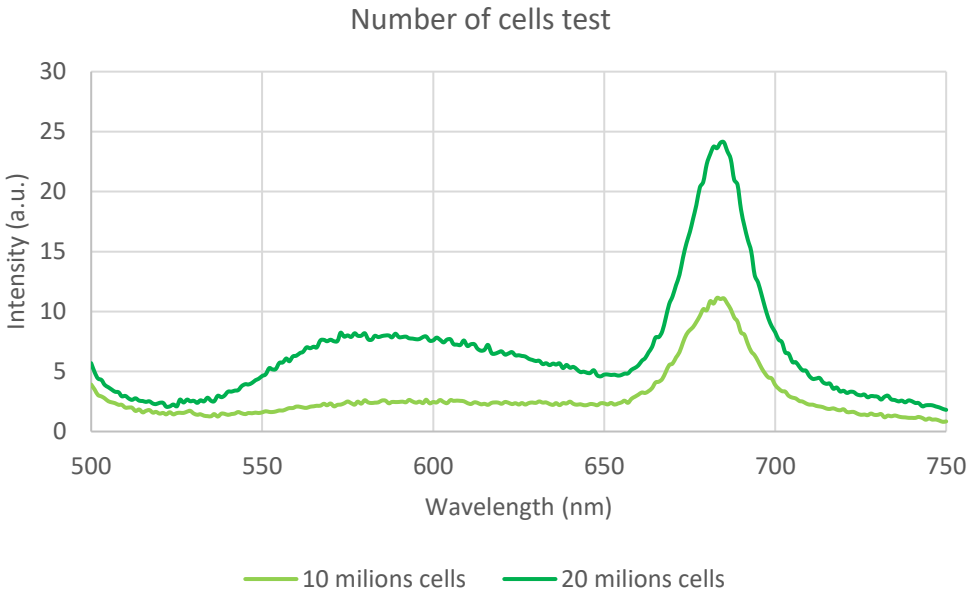

FIGURE 25: Number of cells test. Both samples of *N. gaditana* have the same staining (i.e. 2,6 µg/mL). The green one has a concentration of 20 million of cells while the light green one has a concentration of 10 million of cells. Number of cells significantly influences data making the peaks visible or not

Finally, both incubation time and incubation temperature are essentials for dye penetration and experimental accuracy. But if we kept the temperature constant, we changed the duration, and it showed a smaller impact on the data compared to the effect of cell quantity. The average fluorescence values of Nile red in the 560-610 nm range and chlorophyll in the 680-690 nm range of 20 million of cells are summarized in Table 9.

Time incubation	Neutral lipid	Chlorophyll
10 min	6,00	21,01
15 min	8,16	22,16
20 min	7,65	22,46

TABLE 9: Nile red average intensity (a.u.) in the range between 560-610 and chlorophyll average intensity (a.u.) in the range between 680-690 of 20 million of cells of *N. gaditana* with 2,6 µg/mL of Nile red

These findings collectively contribute to the optimization of the protocol and provide insights into the reliable measurement of neutral lipid content.

4.4 TPT KO mutants neutral lipid content

Following the successful optimization of the protocol, we initiated neutral lipid measurements as detailed in section 3.2.3 to see if the mutants were able to accumulate lipids differently than WT. Initial measurements were conducted on the fluorescence spectrophotometer Cary Eclipse (Agilent Technologies), allowing for a preliminary screening on a larger volume of cells and ensuring the accurate utilization of the TECAN instrument. The data presented here derived from three distinct growth curves, validating our hypothesis regarding the increased accumulation of lipids in mutants compared to the wild type (WT) in low light condition. Indeed, this trend is consistently observed across various days (Figure 26 e 27).

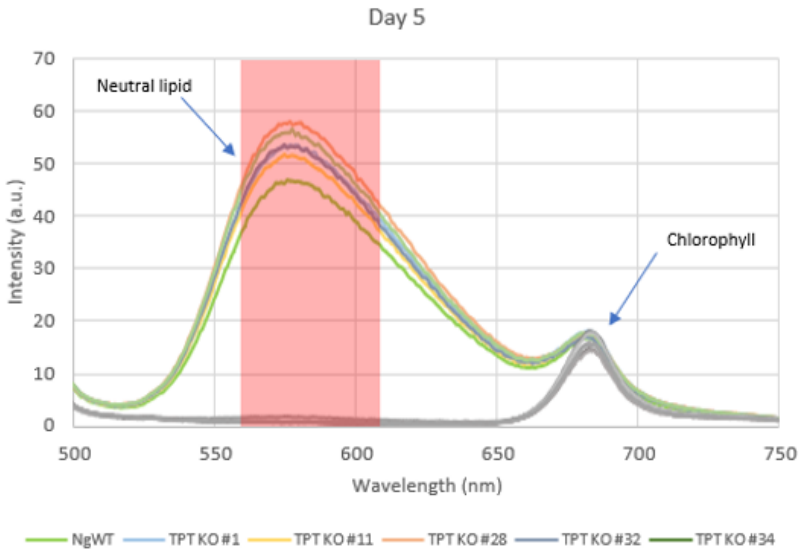

FIGURE 26: Explicative representation of the spectra obtained from the fluorescence spectrophotometer of each line of *N. gaditana* in the day 5 of the growth curve. The red section highlights the wavelength range used for neutral lipids quantification. Left peak represent neutral lipid while right peak represent chlorophyll. All the samples have 20 million of cells with Nile red concentration of 2,6 µg/mL and are stained for 20 minutes. Our hypothesis regarding the increased accumulation of lipids in mutants compared to the wild type (WT) is validate. In a grayscale are represented the spectres of the non-stained cells that have the same peak of the chlorophyll of the stained cells

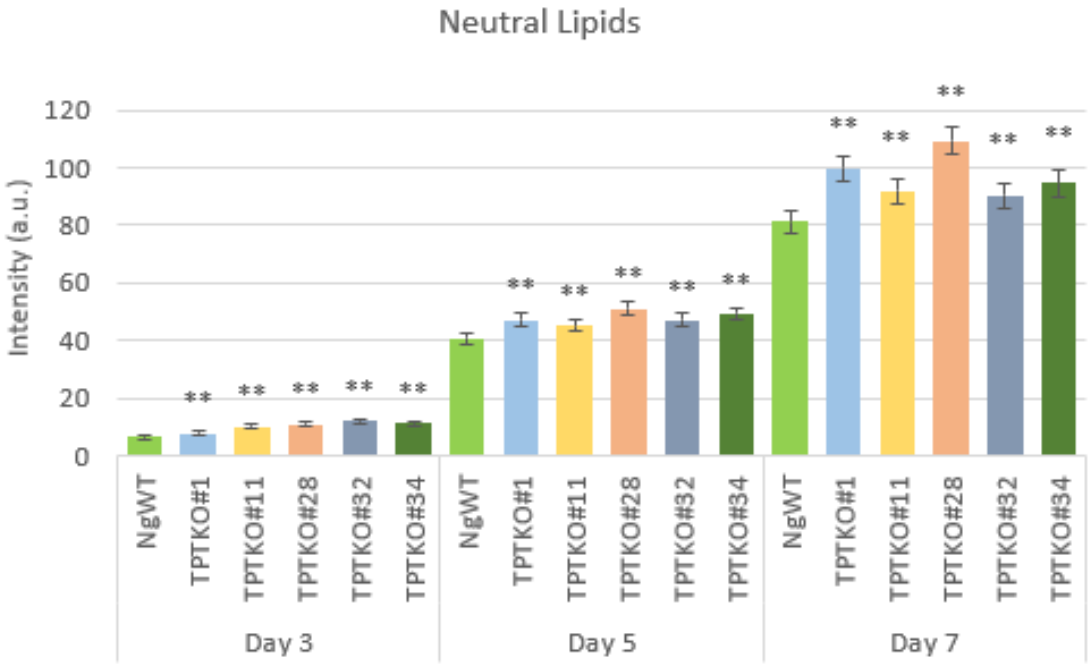

FIGURE 27: Day 3-5-7 average of the Nile red value between 560-610 nm. This value are the average from 3 different curves (6 biological replicates). All *N. gaditana*'s samples have 20 million of cells with Nile red concentration of 2,6 µg/mL and are stained for 20 minutes. ** indicates Anova test with the highest significance (p-value<0,05) between all the lines and the WT for each day. Our hypothesis regarding the increased accumulation of lipids in mutants compared to the wild type (WT) is validate

In Figure 27 it is possible to see how the increase in lipids is constant in each day while maintaining the difference with the WT. On day 7 the difference between mutant lines and WT is maximum.

Subsequent curves involve lipid measurements utilizing the TECAN instrument, enabling a higher number of technical replicates, speeding up the process and subtract less volume from each well for measurements, allowing gas exchanges to remain constant throughout the curve. The data

obtained maintain the same trend, also in the growth curve (Figure 22), and validate the initial hypothesis regarding the increased accumulation of lipids in mutants compared to the wild type, as depicted in Figure 28. This additional figure is derived from two distinct growth curves, providing robust support for the increased lipid accumulation in mutants compared to the WT. Overall, the successful application of both the instruments ensures the reliability and efficiency of the lipid measurement process.

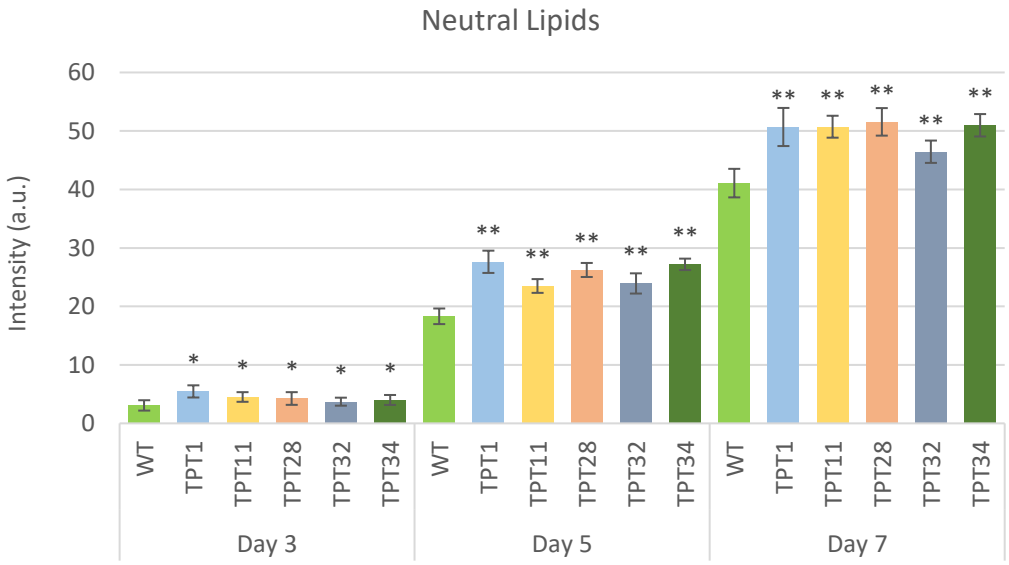

FIGURE 28: Day 3-5-7 average of the Nile red value at TECAN. Gain acquisition to compare the different day is 54. This value are the average from 3 different curves (4 biological replicates). All *N. gaditana*'s samples have 2 million of cells with Nile red concentration of 2,6 µg/mL and are stained for 20 minutes. ** indicates Anova test with the highest significance (p-value<0,05) between all the lines and the WT for each day while * indicates p-value<0,1. Our hypothesis regarding the increased accumulation of lipids in mutants compared to the wild type (WT) is validate.

4.5 *N. oceanica* transformation

For the *Nannochloropsis oceanica* tdTOMATO strain (IMET1) related project, our goal was to perform a transformation to obtain a strain overexpressing a specific desaturase, ultimately improving the fatty acids profile value. In particular, the targeted desaturase is putatively involved in the conversion of ω6 fatty acids to ω3 fatty acids, specifically catalyzing the

transformation of arachidonic acid (C20:4, n-6, ARA, Δ5,8,11,14) into eicosapentaenoic acid (C20:5, n-3, EPA, Δ5,8,11,14,17) (Figure 29).

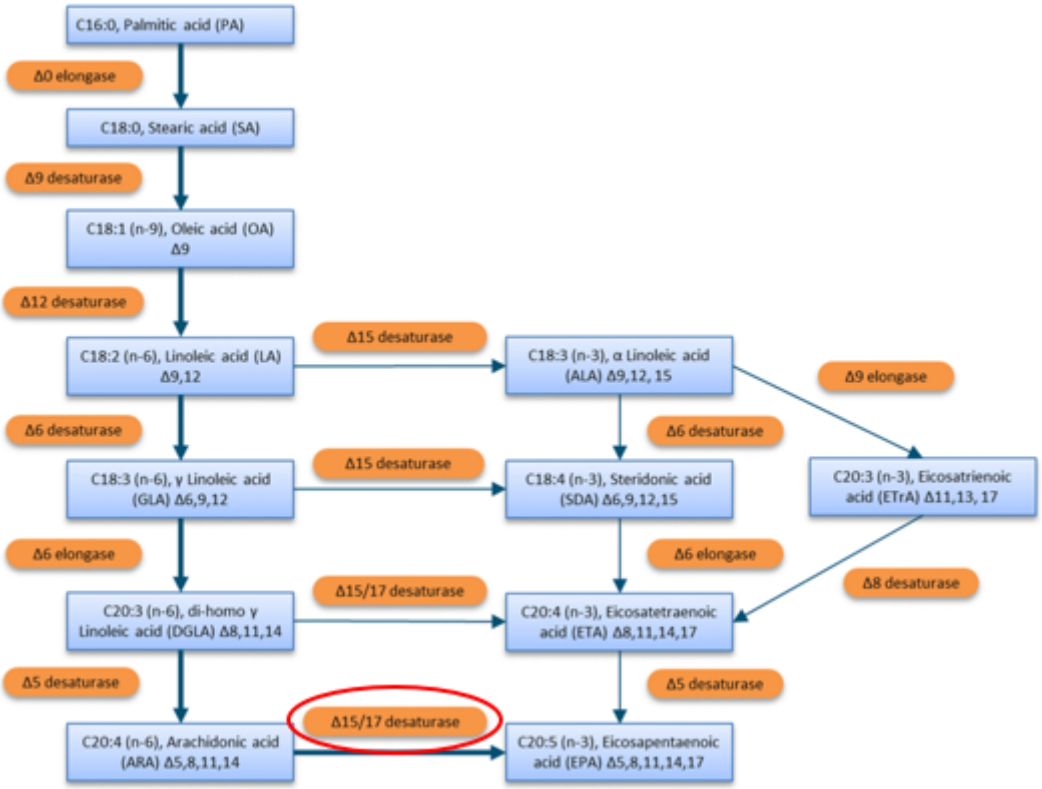

FIGURE 29: General proposed PUFA biosynthesis pathway for *Nannochloropsis* (Jansen et al., 2020). Our putative desaturase is the red circle one and it is involved in converting ω6 fatty acids into ω3 fatty acid, catalyzing the transformation of Arachidonic acid into Eicosapentaenoic acid

Before *N. oceanica* transformation, our first step was to identify the gene for overexpressing the desaturase. To do so, we employed alignment algorithms such as BLAST (https://blast.ncbi.nlm.nih.gov/Blast.cgi) and consulted sequence databases including NCBI (https://www.ncbi.nlm.nih.gov) and NANDESYN (https://nandesyn.single-cell.cn/) (specifically designed for algae). The coding sequence chosen to transform *N. oceanica* is that of a ω3 fatty acid desaturase (ω3FAD, code KY214454) specialized in introducing double bonds at specific positions in the Arachidonic acid. This coding sequence correspond to aminoacid sequence with the code AQX92138[52]. The coding sequence (deprived of

[52] Poliner et al., 'A Toolkit for *Nannochloropsis Oceanica* <span Style="font-Variant'.

introns, Figure 30) was cloned in the optimized plasmid used to transform *N. oceanica* as described in section 3.3.10. Once we obtained the finale plasmid, we sequenced it and found that there are 2 differences between the coding sequence in the database and the one we insert into the plasmid, that are highlighted in violet in Figure 28. They are inside the coding sequence of the enzyme and maybe influence the formation of the same. Further studies are needed to confirm that function is maintained. The final obtained plasmid used for transformation is illustrated in Figure 31.

ACACCAAACAGTTTCGACTTGGCGGCATCTTCTCGGTGACATAACAAACACCGAG
AAAGCCTTTGGACTGATCCTGGCACTCGTTGCCGTGTCATTCCATCTCCAATTCG
GACCTCCAATCAAGCAAGGCTACCCGCTGAATTTAAGCATATAACTAAGCGGAGG
AAAAGAAACTAACCAGGATTCCCCTAGTAACGGCGACAACCAGCTCAGAACTGGA
GCGGACAAGGGGAATCCGACTGTTTAATTAAAACAAAGCATTGCGATGGTCGGAG
ACGATGTTGACGCAATGTGATTTCTGCCCAGTGCTCTGAATGTCAAAGTGAAGGA
ATTCAACCAAGCGCGGGTAAACGGCGGGAGTAACTATGACTCTCTTAAGGTAGCC
AAATGCCTCGTCATCTAATTGGAATGCCCCTCCCCCCTCCCTCCTTCCCTTCATC
CTCCCCTCCGAGCAGGGTGGTACCATGGTTGAGCAAACGTTACCGACCTTGTCCC
AGATCAAGAAAGCCATCCCCGAGAAATGCTTCCAGAAATCCCTCCTCCGCTCCTT
TTACTACATGCTGAGGGACTTCGCGGCCTTGGCGGCACTCTACTTTGTTTATCCC
ACAGTGCAGGCCAAGTATGGATTGCCTGGTTTGTTTGTGTGGTGGAACCTCGCAG
GCTTTTTCATGTGGTGCCTCTTCGTGATAGGCCACGATTGCGGCCATGGCTCCTT
CTCCGAGTACAAGTGGCTCAATGACATATGCGGTCACATTTGCCACGCCCCCTTG
ATGGTGCCTTACTGGCCTTGGCAGAAGTCCCACCGCCTTCACCACATGTACCACA
ACCACCTGACTAAGGACATGTCACACCCGTGGATGACCAAGGAGGTGTTCGAGGA
CTTGACCCCATTCGAGCAGGCGTTGCTGGAGAACCCGCTGTCCCTCTTCATCAAG
TACACCTTCCTTTACCTCTTTGCGGGCAAGATGGATGGCAGCCATGTAGTTCCAT
TCTCCCCCCTCTTCACCGACACCAAGGAGCGGGTGCAATGCGCAGTGTCGACGCT
GGGTATGGTCGTCGCAGGCGCCCTTGTGTACATCGGGCTCGAGGGCGGGAAGGAG
GGAGGGATGGCGAGGATAGGATCCATTTATGTGGTGCCGTTGCTGGTGTTCAATG
CCTGGATCACGATGGTGACATACCTGCAGCACCACGATGAGGACACCAAGGTTTA
TGCAGAGGGGGAGTGGAACTACATCAAGGGGGCCCTGGAGACGATCGACCGCGAA
TACGGCATGGGGATTGACGACCTCTCCCACAATATCACGGATGGCCACGTGGCGC
ACCACCTCTTCTTCACGCAGATCCCGCACTACCACCTGACGGCGGCCACGGCCGC
TGTGAGACAATGCCTGCAACCTACGGGGACCTACAAGAAGAGGAGGAGCTGGAAT
TTTCTCGCTCGTTTCACGGAGCTTAACTACCGTTTGAAATACGTCGCGGGCCAGG
GCGTGCTCTCCTATGTGGATTGGGAGGTCGCTCGCAAGACCCCTGCTTCCGCCGT
CACCTCCTCCTTCTCTTCCTCCTCCTCTTCCTCCCTTCCGGCAGAGGCTGCTGTC
AAGGCGGCTGCTGCCGTTCCCGTTGCTGCTGTTGCTGCTCCCGTCCGAGAAGGAA
GACCAACAAGCAAGCGCTCTCCCACCCGTTCATCCTCCCCTCCGGGTACCGGTCA
TCACCATCACCATCACTGATGGCCAGGGATCAGGAGGAGGGAGTGAAGAGGAGAA
GGGATCTGGTTTCAGAGATCCCCACTTCTGCCGTCGTCTTTCGGCCTTCCTTCCT
TTTAGGTGTCATGCCTTAGGTCCTTCAAGTCCTCACCTGTCGTCGTCATGTGTGT
GTGTGCCCGTCATACAAGTCACTCGATCCAATTCACGCATCGGTTCAATCAAAAT
AAGACTAGACCCCGAGGGAAGAAGGGCAGAAGGAAATCGAAGGGGTGGGATGTGT
GTGAGAGAGGGAAGGAGAAATGAAAGAAGTGAACAATGTCATGGTAGCCAGTAAG

GAGAGAGTAGAAGCGAAGAAAGCAAAAGCACTGTTGTGAAGAAACGAAATGGAAG
ATGGTCATCGCTCCTGGCTCTACTTGTGGTTTTTCTATCTTTAATTTCAGGCGTC
CTGGACTCGTTACATCAGCTCCCTTATCTCATTGGTTTATCCCCTACTCTACTGC
TGCTTCTTCCTTCCATCCGTGACTGTATAACAACGAATTGTAGTACCGCAGATAG
ACAATAGAAAAATGCCAAAAAAGGCATCATTGATTTGCTCCTCCCCATTAAGTCA
CTGTACGCCACCATCGCCACTACCCTCCCTT

Figure 30: Gene coding sequence of the construct introduce in the plasmid. cyano = 25S rDNA fragment; yellow = internal ribosome entry site of *N. oceanica*; blue = tag of 6 Histidine used in affinity column purification; red = α-tubulin terminator; green = CDS of the FADω3; pink = restriction enzyme KpnI site; dark green = mutation between the coding sequence inside the plasmid and the one obtained by database

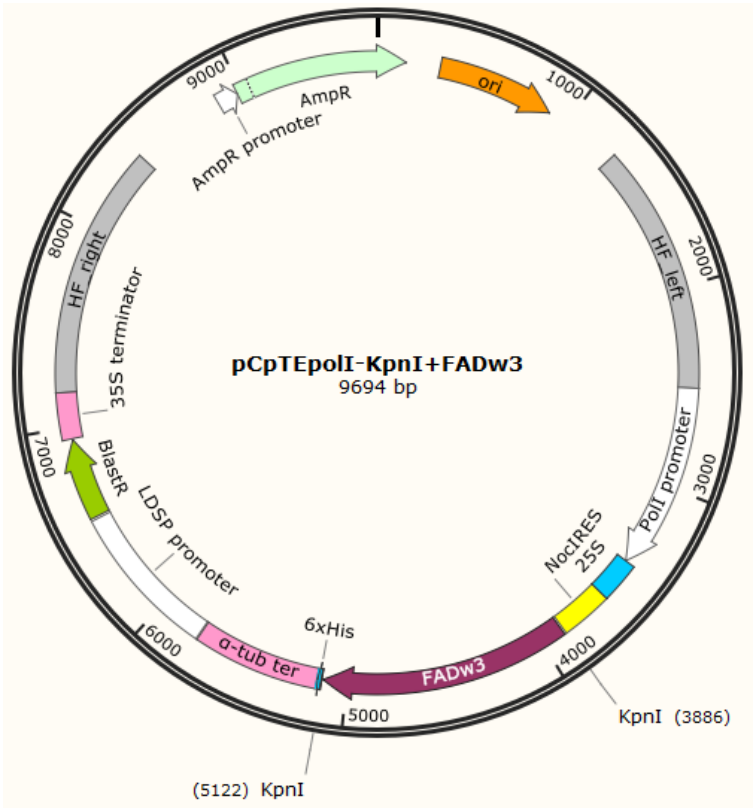

FIGURE 31: pCpTE-polI plasmid used for the transformation of *N. oceanica* to obtain the FADω3 mutant. ori = origin of replication of *E.coli*; AmpR and AmpR promoter = gene and promoter of the gene for ampicillin resistance; PolI promoter = polymerase I translation promoter; 25S = 25S rDNA fragment; NocIRES = internal ribosome entry site of *N. oceanica*; 6xHis = 6 Histidine tag; α-tub ter = α-tubulin terminator; LDSP Prom = promoter of the lipid droplet surface protein; BlastR = gene coding for the resistance to Blasticidin; 35S terminator = translation terminator of 35S gene; HF = homologous region; KpnI = restriction sites used in the cloning strategy are indicated at the sides of the gene; imagine obtained from snapgene

Although this transformation is quite efficient a critical step before transformation involved the linearization of the plasmid portion to be inserted into the genome (Section 3.3.10). This was achieved using the oCST033 and oCST034 primers (refer to Table 10), resulting in shorter linear DNA fragment that facilitates homologous recombination, increasing the frequency of successful integration and eliminates *E. coli* origin of replication and ampicillin resistance (Figure 32).

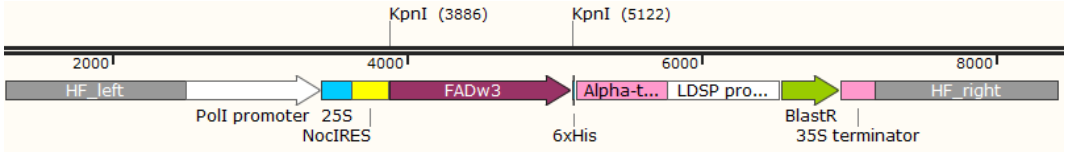

Figure 32: Representative scheme of the linearization product; PolI promoter = polymerase I translation promoter; 25S = 25S rDNA fragment; NocIRES = internal ribosome entry site of *N. oceanica*; 6xHis = 6 Histidine tag; α-tub ter = α-tubulin terminator; LDSP Prom = promoter of the lipid droplet surface protein; BlastR = gene coding for the resistance to Blasticidin; 35S terminator = translation terminator of 35S gene; HF = homologous region; KpnI = restriction sites used in the cloning strategy are indicated at the sides of the gene

The transformation of *N. oceanica* tdTOMATO strain (IMET1) followed the protocol outlined in section 3.4. Linearizing the plasmid proved to be an essential step to enhance the efficiency of recombination e directly on the transformation.

4.6 ω3-FAD mutants genotyping

Before starting genotyping via PCR, an initial screening of the transformed colonies was conducted by selecting mutants through a fluorescence stereomicroscope (Leica MZ16F). To perform transformations, we employed an optimized cloning vector designed for accurate protein localization and gene cloning. The *N. oceanica* IMET1 strain used is optimized for gene insertions (homologous recombination, HR) and facilitates rapid mutant selection. This preliminary check consists in verifying the loss of fluorescence in *N. oceanica* colonies, indicating the disruption of the tdTOMATO gene, thus a successful insertion of the construct into the desired genomic locus (Figure 33 and 34)

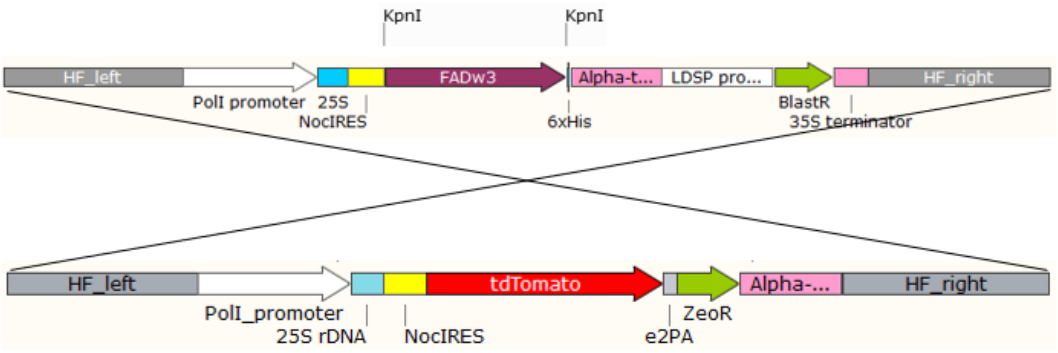

FIGURE 33: Graphic scheme of homologus recombination between the gene constructs FADω3 used to transform the *N. oceanica* and tdTOMATO strain. PolI promoter = polymerase I translation promoter; 25S = 25S rDNA fragment; NocIRES = internal ribosome entry site of N. oceanica; FADω3 = coding sequence of fatty acid desaturase; 6xHis = 6 Histidine tag; α-tub ter = α-tubulin terminator; LDSP Prom = promoter of the lipid droplet surface protein; BlastR = gene coding for the resistance to Blasticidin; 35S ter = translation terminator of 35S gene; HF = homologous region; tdTOMATO = gene for fluorophore tdTOMATO. ZeoR = gene coding for the resistance to Zeocin; KpnI restriction sites used in the cloning strategy are indicated with a small black line.

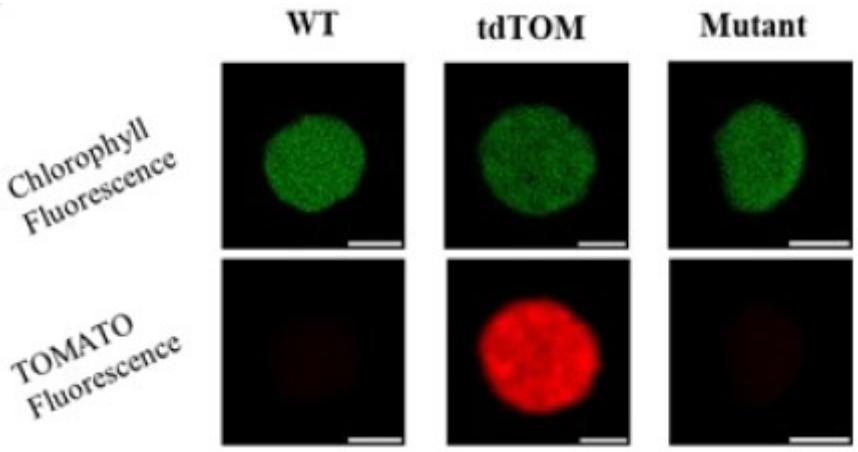

FIGURE 34: Through the red fluorescence loss, the colonies in which the insertion of the construct took place were isolated. Single colonies of N. oceanica WT, tdTOM strain and mutant. Gently provided from Eleonora Mezzadrelli thesis

The microscope fluorescence-based screening resulted in the identification of 15 positive mutants, which were subsequently analysed through PCRs. The genomic DNA was extracted from each mutant, following the procedure outlined in section 3.3.4. A set of primers annealing both on different region of the plasmid and on the target “landing-pad” locus was used (Table 10, Figure 35). Electrophoretic runs on agarose gel (section 3.3.6) were

performed to confirm the potential FADω3 mutants previously identified under the microscope.

Primer	5'-3' sequence
5'-chr3-oCS243	GGATGGGTCTCTTCTCTCTTTCT
oCST033	AGGTAAGGAGTAGGGAGGGG
Seq_ctrl_fw2	TGCCCAGTGCTCTGAATG
NoFADω3-KpnI_fw	TTATGGTACCATGGTTGAGCAAACGTTACC
NoFADω3_fw	ATGGTTGAGCAAACGTTACC
NoFADω3_rv	CGGAGGGGAGGATGAAC
NoFADω3-KpnI-rv	TATAGGTACCCGGAGGGGAGGATGAAC
Seq_ctrl_rv	AGGAAGGCCGAAAGACG
oCS245-Blast_fw	ACGTGTGGGAGAGCGCTTGA
oCS248-Blast_rv	TCAAGCGCTCTCCCACAC
oCST034	TGATTAGTGTGACGGCGGAT
3'-chr3-oCS246	TCTGCGGATGCTGCTACTTTCA

TABLE 10: primers used in molecular biology. Yellow primers were designed by (Südfeld et al., 2021) while the other were designed by us

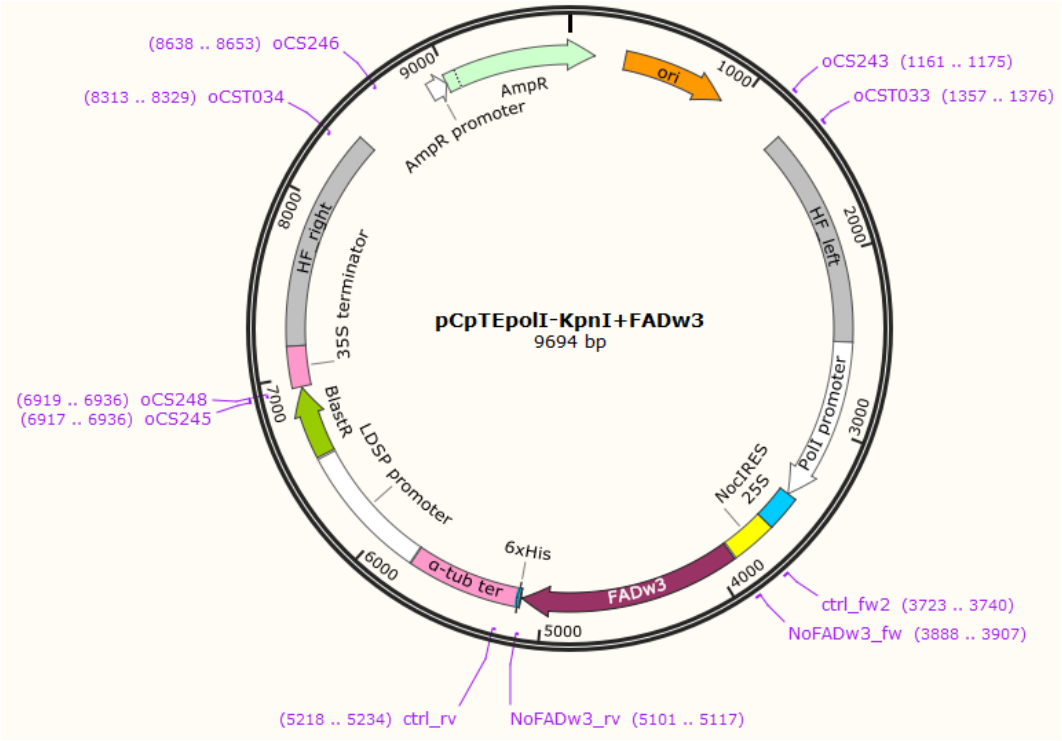

FIGURE 35: plasmid pCpTE-polI with primer. ori = origin of replication of *E.coli*; AmpR and AmpR promoter = gene and promoter of the gene for ampicillin resistance; PolI promoter

= polymerase I translation promoter; 25S = 25S rDNA fragment; NocIRES = internal ribosome entry site of *N. oceanica*; 6xHis = 6 Histidine tag; α-tub ter = α-tubulin terminator; LDSP Prom = promoter of the lipid droplet surface protein; BlastR = gene coding for the resistance to Blasticidin; 35S terminator = translation terminator of 35S gene; HF = homologous region; KpnI = restriction sites used in the cloning strategy are indicated at the sides of the gene; imagine obtained from snapgene

PCR, aimed at verifying the insertion of the gene, was performed using the PFW (primer forward) seq_ctrl_fw2 and PRV (primer reverse) seq_ctrl_rv (Table 10). As shown in Figure 36, the WT exhibited a higher band compared to mutants, suggesting successful insertion.

FIGURE 36: PCR to verify the insertion of the gene; A) Length of the amplified in the ω3FAD construct; B) Length of the amplified in the tdTOMATO construct; C) Electrophoresis run on agarose gel of the PCR; WT exhibited a higher band compared to mutants, suggesting successful insertion

Once we verified the insertion of the construct, and obtain the mutant, further analysis are needed to fully genotyping the line, confirm the functionality of the desaturase we want to over express and to analyse if this overexpression have an impact on the fatty acid profile of the microalgae.

5. Conclusion

This thesis focuses on two crucial aspects, utilizing two distinct microalgae species: *Nannochloropsis gaditana* and *Nannochloropsis oceanica.* The initial focus involved using knockout (KO) mutants of the TPT transporter in *Nannochloropsis gaditana*, achieved through CRISPR-Cas technology. The primary objectives encompassed a dual exploration:

- Understanding the role of the TPT Transporter:
    - Investigating its involvement in cell carbon partitioning and lipid metabolism
    - Assessing the impact of utilize low light intensity on these processes
- Evaluating Mutant Phenotypes:
    - Examining whether mutants exhibited a distinct growth phenotype
    - Investigating their ability to accumulate photosynthates for enhanced cytosolic lipid production compared to the wild type

The growth curves yielded valuable insights into the lipid metabolism of *Nannochloropsis gaditana*, supporting our initial hypothesis to better understand the role of TPT inside the cell and regarding the increased accumulation of lipids in TPT KO mutants compared to the wild type (WT) in low light condition. This condition of light is important because in low light (LL) than to medium light (ML) and high light (HL), DHAP is more abundant than others carbon intermediate and it still an essential molecule in the metabolism, being an intermediate in various metabolic pathways. Also, growth curves were used to ascertain that the mutation in the transporter does not modify the growth of the cells. However, a more in-depth investigation is essential to unravel the intricate mechanisms governing lipid metabolism and the regulation of cell carbon partitioning.

For *Nannochloropsis oceanica*, the aim was the overexpression of a specific ω-3 fatty acid desaturase. The objective was to comprehend this gene function and improve the lipid profile, focusing on the conversion from

arachidonic acid (ARA) to eicosapentaenoic acid (EPA). While successful mutants were obtained, further studies are necessary to validate improvements in the lipid profile and explore potential applications.

Future studies should include comprehensive evaluations to validate these strains for food production. This involves assessing the microalgae's nutritional qualities through biochemical analyses and in vitro experiments to evaluate oil digestibility, bioavailability, and toxicity. Advancements in cultivation, cell breakage, oil production, and processing are crucial for industrialization and scalable cultivation. Adopting biorefinery principles, which optimize industrial processes from both an energy and economic perspective, is a sustainable approach. This strategy aims to extract valuable components for diverse markets, including food, pharmaceuticals, cosmetics, and chemicals.

6.Bibliography

Alboresi, Alessandro, Giorgio Perin, Nicola Vitulo, Gianfranco Diretto, Maryse Block, Juliette Jouhet, Andrea Meneghesso, et al. 'Light Remodels Lipid Biosynthesis in *Nannochloropsis Gaditana* by Modulating Carbon Partitioning between Organelles'. *Plant Physiology* 171, no. 4 (August 2016): 2468–82. https://doi.org/10.1104/pp.16.00599.

Barkia, Ines, Nazamid Saari, and Schonna R. Manning. 'Microalgae for High-Value Products Towards Human Health and Nutrition'. *Marine Drugs* 17, no. 5 (24 May 2019): 304. https://doi.org/10.3390/md17050304.

Basso, Stefania, Diana Simionato, Caterina Gerotto, Anna Segalla, Giorgio M. Giacometti, and Tomas Morosinotto. 'Characterization of the Photosynthetic Apparatus of the Eustigmatophycean Nannochloropsis Gaditana: Evidence of Convergent Evolution in the Supramolecular Organization of Photosystem I'. *Biochimica et Biophysica Acta (BBA) - Bioenergetics* 1837, no. 2 (February 2014): 306–14. https://doi.org/10.1016/j.bbabio.2013.11.019.

Bellou, Stamatia, Mohammed N. Baeshen, Ahmed M. Elazzazy, Dimitra Aggeli, Fotoon Sayegh, and George Aggelis. 'Microalgal Lipids Biochemistry and Biotechnological Perspectives'. *Biotechnology Advances* 32, no. 8 (December 2014): 1476–93. https://doi.org/10.1016/j.biotechadv.2014.10.003.

Caporgno, Martín P., and Alexander Mathys. 'Trends in Microalgae Incorporation Into Innovative Food Products With Potential Health Benefits'. *Frontiers in Nutrition* 5 (31 July 2018): 58. https://doi.org/10.3389/fnut.2018.00058.

Dolganyuk, Vyacheslav, Daria Belova, Olga Babich, Alexander Prosekov, Svetlana Ivanova, Dmitry Katserov, Nikolai Patyukov, and Stanislav Sukhikh. 'Microalgae: A Promising Source of Valuable Bioproducts'. *Biomolecules* 10, no. 8 (6 August 2020): 1153. https://doi.org/10.3390/biom10081153.

Fawcett, Claire A., Gerusa N.A. Senhorinho, Corey A. Laamanen, and John A. Scott. 'Microalgae as an Alternative to Oil Crops for Edible Oils and Animal Feed'. *Algal Research* 64 (May 2022): 102663. https://doi.org/10.1016/j.algal.2022.102663.

Godfray, H. Charles J., John R. Beddington, Ian R. Crute, Lawrence Haddad, David Lawrence, James F. Muir, Jules Pretty, Sherman Robinson, Sandy M. Thomas, and Camilla Toulmin. 'Food Security: The Challenge of Feeding 9 Billion People'. *Science* 327, no. 5967 (12 February 2010): 812–18. https://doi.org/10.1126/science.1185383.

Huang, Weichao, Anagha Krishnan, Anastasija Plett, Michelle Meagher, Nicole Linka, Yongsheng Wang, Bijie Ren, et al. '*Chlamydomonas* Mutants Lacking

Chloroplast TRIOSE PHOSPHATE TRANSPORTER3 Are Metabolically Compromised and Light Sensitive'. *The Plant Cell* 35, no. 7 (26 June 2023): 2592–2614. https://doi.org/10.1093/plcell/koad095.

Janssen, Jorijn H., Jacco Spoelder, Jasper J. Koehorst, Peter J. Schaap, René H. Wijffels, and Maria J. Barbosa. 'Time-Dependent Transcriptome Profile of Genes Involved in Triacylglycerol (TAG) and Polyunsaturated Fatty Acid Synthesis in Nannochloropsis Gaditana during Nitrogen Starvation'. *Journal of Applied Phycology* 32, no. 2 (April 2020): 1153–64. https://doi.org/10.1007/s10811-019-02021-2.

Kusmayadi, Adi, Yoong Kit Leong, Hong-Wei Yen, Chi-Yu Huang, and Jo-Shu Chang. 'Microalgae as Sustainable Food and Feed Sources for Animals and Humans – Biotechnological and Environmental Aspects'. *Chemosphere* 271 (May 2021): 129800. https://doi.org/10.1016/j.chemosphere.2021.129800.

Li-Beisson, Yonghua, Jay J. Thelen, Eric Fedosejevs, and John L. Harwood. 'The Lipid Biochemistry of Eukaryotic Algae'. *Progress in Lipid Research* 74 (April 2019): 31–68. https://doi.org/10.1016/j.plipres.2019.01.003.

Liu, Bingzhi, Zizeng Wang, and Li Feng. 'Effects of Reaction Parameter on Catalytic Hydrothermal Liquefaction of Microalgae into Hydrocarbon Rich Bio-Oil'. *Journal of the Energy Institute* 94 (February 2021): 22–28. https://doi.org/10.1016/j.joei.2020.10.008.

Lubián, Luis M., Olimpio Montero, Ignacio Moreno-Garrido, I. Emma Huertas, Cristina Sobrino, Manuel González-del Valle, and Griselda Parés. '[No Title Found]'. *Journal of Applied Phycology* 12, no. 3/5 (2000): 249–55. https://doi.org/10.1023/A:1008170915932.

Ma, Xiao-Nian, Tian-Peng Chen, Bo Yang, Jin Liu, and Feng Chen. 'Lipid Production from Nannochloropsis'. *Marine Drugs* 14, no. 4 (25 March 2016): 61. https://doi.org/10.3390/md14040061.

Maeda, Yoshiaki, Tomoko Yoshino, Tadashi Matsunaga, Mitsufumi Matsumoto, and Tsuyoshi Tanaka. 'Marine Microalgae for Production of Biofuels and Chemicals'. *Current Opinion in Biotechnology* 50 (April 2018): 111–20. https://doi.org/10.1016/j.copbio.2017.11.018.

Meneghesso, Andrea, Diana Simionato, Caterina Gerotto, Nicoletta La Rocca, Giovanni Finazzi, and Tomas Morosinotto. 'Photoacclimation of Photosynthesis in the Eustigmatophycean Nannochloropsis Gaditana'. *Photosynthesis Research* 129, no. 3 (September 2016): 291–305. https://doi.org/10.1007/s11120-016-0297-z.

Nellemann, C., United Nations Environment Programme, and GRID--Arendal, eds. *The Environmental Food Crisis: The Environment's Role in Averting Future Food Crises: A UNEP Rapid Response Assessment*. Arendal, Norway: UNEP, 2009.

Ouellette, Robert J., and J. David Rawn. *Organic Chemistry: Structure, Mechanism, and Synthesis*. Amsterdam: Elsevier, 2014.

Paul Abishek, Monford, Jay Patel, and Anand Prem Rajan. 'Algae Oil: A Sustainable Renewable Fuel of Future'. *Biotechnology Research International* 2014 (5 May 2014): 1–8. https://doi.org/10.1155/2014/272814.

Poliner, Eric, Jane A. Pulman, Krzysztof Zienkiewicz, Kevin Childs, Christoph Benning, and Eva M. Farré. 'A Toolkit for *Nannochloropsis Oceanica* CCMP 1779 Enables Gene Stacking and Genetic Engineering of the Eicosapentaenoic Acid Pathway for Enhanced Long-chain Polyunsaturated Fatty Acid Production'. *Plant Biotechnology Journal* 16, no. 1 (January 2018): 298–309. https://doi.org/10.1111/pbi.12772.

Radakovits, Randor, Robert E. Jinkerson, Susan I. Fuerstenberg, Hongseok Tae, Robert E. Settlage, Jeffrey L. Boore, and Matthew C. Posewitz. 'Draft Genome Sequence and Genetic Transformation of the Oleaginous Alga Nannochloropsis Gaditana'. *Nature Communications* 3, no. 1 (21 February 2012): 686. https://doi.org/10.1038/ncomms1688.

Ravindran, Balasubramani, Sanjay Gupta, Won-Mo Cho, Jung Kim, Sang Lee, Kwang-Hwa Jeong, Dong Lee, and Hee-Chul Choi. 'Microalgae Potential and Multiple Roles—Current Progress and Future Prospects—An Overview'. *Sustainability* 8, no. 12 (25 November 2016): 1215. https://doi.org/10.3390/su8121215.

Razeghifard, Reza. 'Algal Biofuels'. *Photosynthesis Research* 117, no. 1–3 (November 2013): 207–19. https://doi.org/10.1007/s11120-013-9828-z.

Ritchie, Hannah, Pablo Rosado, and Max Roser. 'Environmental Impacts of Food Production', n.d. 'https://ourworldindata.org/environmental-impacts-of-food'.

Rumin, Judith, Hubert Bonnefond, Bruno Saint-Jean, Catherine Rouxel, Antoine Sciandra, Olivier Bernard, Jean-Paul Cadoret, and Gaël Bougaran. 'The Use of Fluorescent Nile Red and BODIPY for Lipid Measurement in Microalgae'. *Biotechnology for Biofuels* 8, no. 1 (December 2015): 42. https://doi.org/10.1186/s13068-015-0220-4.

Santos-Sánchez, N. F., R. Valadez-Blanco, B. Hernández-Carlos, A. Torres-Ariño, P. C. Guadarrama-Mendoza, and R. Salas-Coronado. 'Lipids Rich in ω-3 Polyunsaturated Fatty Acids from Microalgae'. *Applied Microbiology and Biotechnology* 100, no. 20 (October 2016): 8667–84. https://doi.org/10.1007/s00253-016-7818-8.

Südfeld, Christian, Ana Pozo-Rodríguez, Sara A. Manjavacas Díez, René H. Wijffels, Maria J. Barbosa, and Sarah D'Adamo. 'The Nucleolus as a Genomic Safe Harbor for Strong Gene Expression in Nannochloropsis Oceanica'. *Molecular Plant* 15, no. 2 (February 2022): 340–53. https://doi.org/10.1016/j.molp.2021.11.003.

Turchetto-Zolet, Andreia Carina, Ana Paula Christoff, Franceli Rodrigues Kulcheski, Guilherme Loss-Morais, Rogerio Margis, and Marcia Margis-Pinheiro. 'Diversity and Evolution of Plant Diacylglycerol Acyltransferase (DGATs) Unveiled by Phylogenetic, Gene Structure and Expression Analyses'. *Genetics and Molecular Biology* 39, no. 4 (3 October 2016): 524–38. https://doi.org/10.1590/1678-4685-gmb-2016-0024.

Van Der Spiegel, M., M.Y. Noordam, and H.J. Van Der Fels-Klerx. 'Safety of Novel Protein Sources (Insects, Microalgae, Seaweed, Duckweed, and Rapeseed) and Legislative Aspects for Their Application in Food and Feed Production'. *Comprehensive Reviews in Food Science and Food Safety* 12, no. 6 (November 2013): 662–78. https://doi.org/10.1111/1541-4337.12032.

Xue, Zhaohui, Shihao Li, Wancong Yu, Xin Gao, Xu Zheng, Yue Yu, and Xiaohong Kou. 'Research Advancement and Commercialization of Microalgae Edible Oil: A Review'. *Journal of the Science of Food and Agriculture* 101, no. 14 (November 2021): 5763–74. https://doi.org/10.1002/jsfa.11390.